

Smartphone based Colour Ratio Pyrometry for Flame Temperature Measurement

Submitted in partial fulfillment of
the degree of

Dual(B.Tech + M.Tech) degree

by
Tejas Sakhalkar
Roll no. 18D170032

Supervisor(s):

Prof. Asish Kumar Sarangi (Guide)
Prof. Neeraj Kumbhakarna (Co-guide, ME)



Department of Energy Science and Engineering

Indian Institute of Technology, Bombay

2023

Thesis Approval

The thesis entitled
Smartphone based Colour Ratio Pyrometry for Flame Temperature Measurement
by
Tejas Dattatray Sakhalkar
18D170032
is approved for the degree of Dual (B.Tech + M.Tech) Degree



27/6/23

Examiner-1



27/6/23

Examiner-2



27/6/23

Guide



27/6/23

Co-guide



Chairperson

Date: 27/6/2023

Place: Mumbai

Acknowledgement

I would like to extend my deepest gratitude to my esteemed project guide, Professor Asish Kumar Sarangi, and co-guide, Professor Neeraj Kumbhakarna, for their invaluable guidance, unwavering attention, insightful suggestions, and support throughout the duration of this project. Their expertise and encouragement have been instrumental in shaping the outcome of this research endeavor.

I would also like to express my heartfelt appreciation to Mr. Khokan Sahoo, a Ph.D. student in the Aerospace Department, and Mr. Utkarsh Gupta, a junior Dual Degree student from the ME department, for their generous assistance in the areas of droplet combustion and flat flame setup, respectively. I am sincerely grateful to Ms. Priyadarshini Kamat, a junior DD student from the DESE department, for her invaluable support in managing the practical aspects and other complexities associated with the DDP-related work. Her assistance has been indispensable in ensuring the smooth progression of this research.

I would like to acknowledge the support of my fellow batchmates and friends, Mr. Anmol Gupta, Mr. Nikhil Sapkale, and Mr. Miriyala Sagar, who graciously provided their smartphones equipped with raw image capability whenever it was required. Their willingness to lend a hand has been instrumental in capturing crucial data for this project. A special mention goes to Mr. Rahul, the diligent lab technician, whose expertise and assistance were pivotal in setting up the devices in the IC Engine Lab and Fluid Power Lab.

Furthermore, I am indebted to the senior students from the IC Engine and Combustions Lab for their generous support in addressing the challenges encountered during the experimental setup for combustion. Lastly, I would like to express my sincere gratitude to all individuals who have directly or indirectly contributed to the development of this project. Your assistance, whether through discussions, feedback, or general support, has played a crucial role in shaping the outcome of this research.

I would also like to extend a special appreciation to my loving parents, whose unwavering support and encouragement have been the driving force behind my journey. Their presence throughout the ups and downs of this endeavor has been an endless source of inspiration.

Thank you all for your immense contributions and support, without which this project would not have been possible.

Date : 20 June 2023

Tejas Sakhalkar

Declaration

I declare that this report, submitted in partial fulfillment of the requirements of the Dual Degree Project- Stage II is a record of work carried out by me under the supervision of project guide Prof. Asish Sarangi and co-guide Prof. Neeraj Kumbhakarna. I declare that this written submission represents my ideas in my own words, and where others' ideas or words have been included, I have adequately cited and referenced the sources.

I also declare that I have adhered to all academic honesty and integrity principles and have not misrepresented, fabricated, or falsified any idea/data/fact/source in my submission. I understand that any violation of the above will cause disciplinary action by the Institute and can also evoke penal action from the sources which have thus not been appropriately cited or from whom proper permission has not been taken when needed.

Date : 20 June 2023

Name: Tejas Sakhalkar

Place : IIT Bombay, Mumbai

Roll No: 18D170032

Abstract

Flame temperature measurement, employing pyrometry or flame spectroscopy techniques, plays a vital role in a wide range of applications, including furnace operations, laboratory experiments, and understanding reaction energetics. While various methods have been developed for flame temperature measurement, each technique has its own advantages and limitations. This thesis focuses on investigating the colour ratio pyrometry technique and explores the feasibility of utilizing smartphone cameras as an alternative to conventional optical sensors to develop a user-friendly product.

The primary objective of this research is to develop a smartphone application capable of analyzing flame temperature based on captured RAW images. To achieve this, the underlying principles of colour ratio pyrometry and its applicability in flame temperature measurement are discussed in this thesis. Furthermore, the development process of the smartphone application, including the necessary image processing algorithms and calibration procedures are discussed. Experimental validation of the application is conducted using controlled flame sources with known temperatures. The accuracy and reliability of the smartphone-based colour ratio pyrometry approach are assessed by comparing the results obtained from the application with those obtained using established techniques and reference measurements.

The findings of this research demonstrate the potential of utilizing smartphone cameras for flame temperature analysis by colour ratio pyrometry. The developed application provides a convenient and cost-effective solution for individuals and professionals requiring quick and reliable flame temperature measurements in various settings.

Keywords: Flame temperature, Pyrometry, CRP, Sooty flame, Android app, Thermometry, Non-intrusive technique, Spectroscopy, Product development, Raspberry Pi, Spectral Response Curve

Contents

| | |
|--|-----------|
| 1 Introduction | 1 |
| 1.1 Background and motivation | 1 |
| 1.2 Objectives | 3 |
| 1.3 Methodology and Organization of the Thesis | 3 |
| 2 Pyrometry | 5 |
| 2.1 Measurement Techniques | 5 |
| 2.1.1 Thermocouple | 6 |
| 2.1.2 Rayleigh thermometry | 8 |
| 2.1.3 CARS | 9 |
| 2.1.4 Interferometry | 11 |
| 2.1.5 Infrared (IR) camera | 11 |
| 2.1.6 Thin Filament Pyrometry | 13 |
| 2.1.7 Soot pyrometry | 14 |
| 2.2 Two-colour Pyrometry | 14 |
| 2.2.1 Principle of Two-colour Pyrometry | 14 |
| 2.2.2 Implementation of Two-colour Pyrometry | 15 |
| 2.2.3 Advantages of Two-colour Pyrometry | 16 |
| 2.2.4 Hottel and Broughton Approach | 16 |
| 2.2.5 Comparison with colour-ratio pyrometry | 17 |
| 2.3 Colour Ratio Pyrometry | 18 |
| 3 Imaging Technology | 21 |
| 3.1 Camera sensors | 21 |
| 3.1.1 CCD (Charge-Coupled Device) | 21 |
| 3.1.2 CMOS (Complementary Metal-Oxide-Semiconductor) | 23 |
| 3.2 Bayer Filter | 25 |

| | |
|--|-----------|
| 3.2.1 The Purpose of the Bayer Filter | 25 |
| 3.2.2 Bayer Filter Pattern | 26 |
| 3.2.3 Colour Reconstruction | 26 |
| 3.2.4 Challenges and Limitations | 26 |
| 3.2.5 Alternative Colour Filter Arrays | 27 |
| 3.3 Threshold Levels | 27 |
| 3.3.1 Black Level | 27 |
| 3.3.2 White Level | 28 |
| 3.4 DSLR Camera | 28 |
| 3.4.1 History of DSLR Cameras | 28 |
| 3.4.2 Current Technology of DSLR Cameras | 29 |
| 3.5 Phone Camera Sensors | 30 |
| 3.5.1 History of Phone Camera Sensors | 30 |
| 3.5.2 Current Technology of Phone Camera Sensors | 30 |
| 3.6 Parameters in cameras | 31 |
| 3.6.1 ISO | 31 |
| 3.6.2 Shutter Speed | 32 |
| 3.6.3 Aperture | 32 |
| 3.6.4 White Balance | 33 |
| 3.6.5 Focus Modes | 33 |
| 3.7 Image File Format | 34 |
| 3.7.1 JPEG | 34 |
| 3.7.2 RAW | 34 |
| 3.7.3 TIFF | 34 |
| 3.7.4 DNG | 34 |
| 3.8 Camera APIs(Application programming interface) | 35 |
| 3.8.1 CameraAPI | 35 |
| 3.8.2 CameraAPI2 | 35 |
| 3.8.3 Comparison | 36 |
| 3.9 Importance of RAW format | 36 |
| 3.10 Sensors used in this study | 38 |
| 4 Experimental Setups | 39 |

| | |
|---|-----------|
| 4.1 Monochromator setup | 39 |
| 4.1.1 Monochromator | 40 |
| 4.1.2 Power meter | 40 |
| 4.1.3 Sensor Calibration | 42 |
| 4.1.4 Calibration Curves | 44 |
| 4.2 Candle Flame setup | 48 |
| 4.3 Blackbody Furnace Setup | 50 |
| 4.4 Flat Flame Setup | 52 |
| 4.5 Droplet setup | 58 |
| 4.6 Dry Block thermocouple calibration setup | 60 |
| 5 Product development | 62 |
| 5.1 Milestones in the product development process | 64 |
| 5.1.1 Applications developed while learning | 64 |
| 5.1.2 Models worked on while learning | 65 |
| 5.2 RPi Product | 66 |
| 5.3 Final application | 67 |
| 6 Conclusions | 71 |
| Appendices | 73 |
| A | 74 |
| A.1 Matlab code for CRP | 74 |
| A.1.1Part 1 of the code | 74 |
| A.1.2Part 2 | 78 |
| A.2 Functions used in the code | 83 |
| B | 86 |
| B.1 RPi code to capture raw image | 86 |
| C | 88 |
| C.1 Edge Detection | 88 |

List of Figures

| | |
|---|----|
| 2.1 K-type thermocouple schematic [5] | 7 |
| 2.2 Rayleigh thermometry in combustor [7] | 9 |
| 2.3 CARS technique [8] | 10 |
| 2.4 Michelson interferometer [10] | 12 |
| 2.5 Thin filament pyrometry [11] | 13 |
| 2.6 Two colour Pyrometry Setup [14] | 15 |
| 2.7 Wien's displacement law(formulated by German physicist Wilhelm Wien in 1893) [19] | 19 |
| 3.1 CCD camera sensor [22] | 22 |
| 3.2 CMOS camera sensor [22] | 23 |
| 3.3 Bayer Filter [25] | 25 |
| 3.4 DSLR Camera schematic [27] | 29 |
| 3.5 Phone camera sensor [28] | 30 |
| 3.6 Non linearity in exposure time if JPG images are used instead of raw images | 37 |
| 4.1 HO-SP-SQR200F monochromator [33] | 41 |
| 4.2 HO-OPM-01UV optical power meter [35] | 41 |
| 4.3 Measured absorbance of ND filter with OD of 2 | 44 |
| 4.4 Exposure Time Linearity Check of Sensor 3 | 44 |
| 4.5 ISO Linearity Check of Sensor 3 | 45 |
| 4.6 White Balance Linearity Check of Sensor 3 | 45 |
| 4.7 Spectral Response curve of CANON EOS 550D camera [1] | 46 |
| 4.8 Spectral Response Curve of Sensor 1 | 46 |
| 4.9 Spectral Response Curve of Sensor 2 | 47 |
| 4.10 Spectral Response Curve of Sensor 3 | 47 |
| 4.11 Spectral Response Curve of Sensor 4 | 47 |

| | |
|---|----|
| 4.12 Monochromator light captured by Sensor 2 | 48 |
| 4.13 CRP Results using Canon EOS 550D [1] | 49 |
| 4.14 Candle flame image and the temperature distribution without Abel inversion | 50 |
| 4.15 Distribution of temperature along horizontal axis through the centre of flame | 50 |
| 4.16 Calsys 1500BB Blackbody Furnace [39] | 52 |
| 4.17 Mckenna Burner Schematic [2] | 55 |
| 4.18 Variation of temperature along vertical axis of flat flame | 55 |
| 4.19 Flat flame and the temperature distribution | 56 |
| 4.20 NASA CEA simulation results- a variation of adiabatic flame temperature with equivalence ratio | 56 |
| 4.21 Change in flame structure with variation in shield gas flow rate (lpm): 2.5, 5, 7.5, 10 | 57 |
| 4.22 Blue flat flame with an equivalence ratio of 1.5 | 58 |
| 4.23 The raw phone camera images of coal tar pitch and RP1 surrogate fuel droplet flame | 59 |
| 4.24 Temperature distribution of coal tar pitch flame and RP1 surrogate fuel flame | 59 |
| 4.25 Fluke Calibration 9173 dry-block calibrator [45] | 61 |
| | |
| 5.1 Applications created while learning the various methods of android app development | 65 |
| 5.2 Deep learning on Android application using MATLAB Simulink . . . | 65 |
| 5.3 Digit Prediction on Android application using MATLAB Simulink-block1 | 66 |
| 5.4 Digit Prediction on Android application using MATLAB Simulink-block2 | 66 |
| 5.5 Future possibility of advanced Android App | 68 |
| 5.6 Screen 1 of the Matlab app | 69 |
| 5.7 Screen 2 of the Matlab app | 69 |
| 5.8 Result page of the Matlab app | 70 |

List of Tables

| | |
|---|----|
| 2.1 Types of thermocouples | 7 |
| 3.1 Sensors used in the study | 38 |
| 4.1 Variation in flame temperature with equivalence ratio | 57 |

Nomenclature and Symbols

| Symbol | Symbol Description |
|------------|---|
| I | Intensity of light |
| λ | Wavelength |
| T | Temperature |
| ϵ | Emissivity |
| h | Planck's constant |
| c | Velocity of light |
| k | Boltzmann constant |
| CRP | colour Ratio Pyrometry |
| α | Soot dispersion exponent |
| LSD | Laser schlieren deflectometry |
| EM | Electromagnetic |
| PM | Particulate Matter |
| EMF | ElectroMotive Force |
| ω | Angular Frequency |
| CARS | Coherent Anti-Stokes Raman Spectroscopy |
| CCD | Charged Coupled Device |
| CMOS | Complementary Metal Oxide Semiconductor |
| DSLR | Digital Single-Lens Reflex |
| TIFF | Tag Image File Format |
| SRC | Spectral Response Curve |
| DNG | Digital Negative Image |
| ND | Neutral Density |
| OD | Optical Density |
| RGB | Red, Green, Blue |
| RPi | Raspberry Pi |
| η | Signal |

Chapter 1

Introduction

1.1 Background and motivation

Measuring the temperature is one of the most commonly used tools in engineering laboratories to factories and research institutes. From the thermometers that we use at our home to the thermocouples made of exotic materials used to measure very high flame temperatures, various types of instruments are used to measure the temperatures. Because of very high temperatures, the measurements of flame temperature require special techniques. The devices that can measure such temperatures are called pyrometers. This measurement is essential to know:

1. Efficiency of combustion
2. Design of the reactions
3. Emissions (such as oxides of nitrogen, NO_x, particulate matter, PM, partial combustion products)
4. Formation mechanisms of chemical reactions

The techniques used for flame temperature measurement are thermocouple, Rayleigh thermometry, CARS, interferometry, thin filament pyrometry, soot pyrometry, etc. In most of the techniques, soot acts as an error-generating entity, but soot pyrometry heavily depends on the radiation by soot particles inside the flame to measure the temperature. The technique provides other advantages, like the determination of the correct temperature if a signal gets weaker independent of the wavelength. The two techniques based on soot pyrometry, two-colour pyrometry, and colour-ratio pyrometry, use optical sensors to measure the intensity of specific wavelengths emitted by a flame and then computes the temperature of the flame from these readings.

There has been various research work done on the method of colour ratio pyrometry using DSLR cameras as optical sensors. Anand[1], in his paper on droplet combustion, studied this technique to measure the flame temperature as well as the soot fraction in the flame. His work was based on the combustion behavior of novel BHC fuels and quantifying the temperature and sooting propensities of these compounds. A commercially available DSLR (digital single-lens reflex) camera was calibrated for measuring temperature using the colour-ratio pyrometry (CRP) technique. Temperature profiles, estimated using CRP, were validated with a blackbody radiation source. This technique was then tested on a candle flame, a droplet flame and an ethylene-air flat flame stabilized on a McKenna burner.

This work was continued by Ansari[2] as a Masters' thesis. In his work, smartphone and DSLR cameras were calibrated for CRP techniques. The calibration was done by extracting the camera's spectral response curve (SRC). The SRCs obtained from three different smartphones were extracted and generalized using skew-normal distribution.

1.2 Objectives

- Investigate the colour ratio pyrometry technique for flame temperature measurement and understand its underlying principles.
- Explore the feasibility of utilizing smartphone cameras as an alternative to conventional optical sensors, such as DSLRs, for flame temperature analysis.
- Develop a smartphone application capable of capturing and analyzing raw images to determine flame temperature.
- Implement image processing algorithms and calibration procedures within the smartphone application to accurately calculate flame temperature based on colour ratios.
- Conduct experimental validation of the smartphone-based colour ratio pyrometry approach using controlled flame sources with known temperatures.
- Compare the results obtained from the smartphone application with those obtained using established flame temperature measurement techniques and reference measurements to assess accuracy and reliability.
- Demonstrate the potential of utilizing smartphone cameras and the developed application as a convenient and cost-effective solution for flame temperature analysis in various settings.
- Provide a comprehensive understanding of the strengths and limitations of smartphone-based colour ratio pyrometry for flame temperature measurement.
- Identify areas for further improvement and future research in smartphone-based flame temperature analysis.

1.3 Methodology and Organization of the Thesis

The second chapter focuses on the measurement techniques used for flame temperature analysis, with a detailed study of various methods and their respective advantages and

disadvantages. In particular, two techniques, namely two-colour pyrometry and colour ratio pyrometry, are examined in depth, including their mathematical formulations for temperature calculation. This chapter, titled "Measurement Techniques," sets the foundation for the subsequent chapters.

Moving on to the third chapter, the emphasis shifts to imaging technology, which plays a crucial role in implementing the colour ratio pyrometry method. In this chapter, a comprehensive analysis is conducted on different camera sensors, such as CCD and CMOS, along with their distinctive features like Bayer Filter and Extremum Levels. A thorough investigation of DSLR and phone cameras is also conducted, considering various image file formats and camera application programming interfaces (APIs). This exploration of imaging technology is essential for understanding the subsequent experimental procedures.

Chapter four delves into the practical implementation of the colour ratio pyrometry method. To begin, the various sensors used in the study are calibrated, including phone camera sensors and the RPi camera module sensor. Subsequently, the method is tested on different types of flames, such as candle flames, McKenna burner flames, and droplet flames. This chapter, titled "Experimental Work," provides detailed information about the setups and procedures employed during the experiments.

The fifth chapter is dedicated to product development, where the entire procedure is transformed into a user-friendly app-based product. Multiple platforms are explored, and various codes are written to achieve this goal. The appendix section contains the codes for reference. This chapter, "Product Development," demonstrates the practical application of the research findings.

Finally, the conclusions derived from the study are presented in the sixth chapter, titled "Conclusions." Here, the key findings, limitations, and potential areas for future research are discussed, providing a comprehensive summary of the thesis.

Chapter 2

Pyrometry

2.1 Measurement Techniques

The devices used for flame temperature measurement are classified into two categories:

1. **Intrusive**- Intrusive means something that is inserted. In this case, intrusive means the devices that are inserted inside
2. **Non-intrusive**- These kinds of devices are not directly inserted into the flame but use the EM emissions from the flame or use external waves to measure the flame

temperature. One such technique uses laser beams to detect the temperature of the flame. [3]

2.1.1 Thermocouple

Thermocouples are commonly used in various industries and applications for temperature measurement. They operate on the principle of the Seebeck effect, which states that when two dissimilar metals are joined at two different temperatures, a voltage is generated across the junction.

The basic construction of a thermocouple consists of two wires made of different metals, typically known as the positive and negative legs. These wires are welded together at one end to form the hot junction, which is exposed to the temperature being measured. The other ends of the wires are connected to a measuring instrument or a data acquisition system.

When there is a temperature gradient between the hot junction and the other end of the thermocouple, a voltage is produced due to the difference in Seebeck coefficients of the two metals. The Seebeck coefficient is a material-specific property that determines the magnitude of the voltage generated for a given temperature difference.

The voltage generated by the thermocouple is directly proportional to the temperature difference between the hot junction and the reference end. Therefore, by measuring the voltage, the temperature can be determined using a calibration curve or an appropriate equation for the specific thermocouple type. (see figure 2.1)

One of the advantages of thermocouples is their ability to measure a wide range of temperatures, from cryogenic temperatures to extremely high temperatures. Different types of thermocouples are available, each with its own temperature range and characteristics, such as type K, type J, type T, and type E, among others.

Thermocouples are widely used in industrial processes, heating and cooling systems, automotive applications, and scientific research. They are relatively inexpensive, rugged, and can withstand harsh environments. However, it's important to note that thermocouples are intrusive measurement devices, as they require direct contact with the medium being measured. The accuracy of flame temperature measurements using thermocouples is constrained by several factors. These include heat losses from the thermocouple bead, uncertainties in estimating flame emissivity, and the potential deposition of soot on the thermocouple bead. [4]

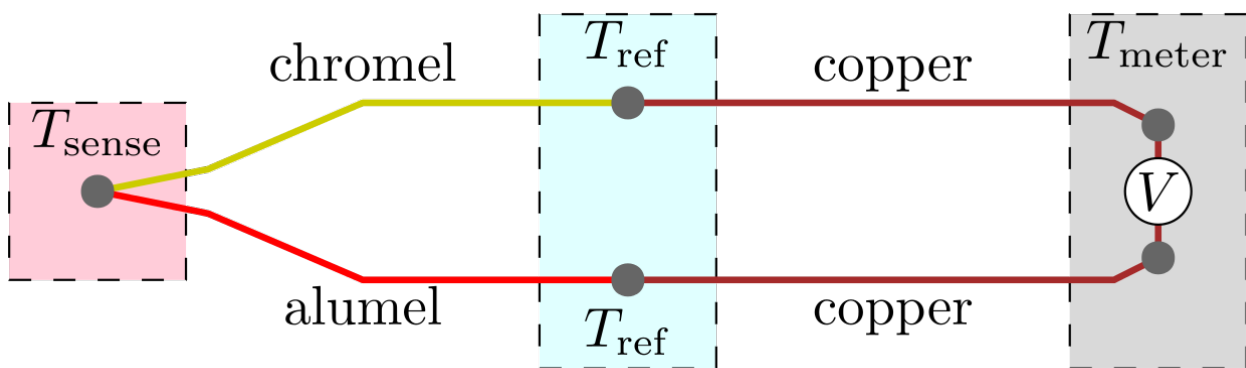


Figure 2.1: K-type thermocouple schematic [5]

Based on the metal pair used, the thermocouples are divided into many classes as mentioned in Table 2.1.

Table 2.1: Types of thermocouples

| Type | Metals | Sensitivity | Operating Range | Application |
|------|------------------------|-------------|---------------------|---------------------------------|
| E | Chromel-constantan | 68uV/C | -270 °C to +740 °C | Cryogenic use |
| J | Iron-Constantan | 50uV/C | -40 °C to +750 °C | Higher sensitivity than K |
| K | Chromel-Alumel | 41uV/C | -200 °C to +1350 °C | Cheap |
| B | 70%Pt/30%Rh–94%Pt/6%Rh | NA | 50 to 1800 °C | High Temperature |
| R | 87%Pt/ 13%Rh–Pt | NA | 0 to 1600 °C | Stable |
| S | 90%Pt/ 10%Rh–Pt | NA | 0 to 1600 °C | Practical standard thermometers |

NA: Not Available

2.1.2 Rayleigh thermometry

Rayleigh thermometry is a technique that utilizes the principles of Rayleigh scattering to measure the temperature of combustion gases. Rayleigh scattering refers to the scattering of light by particles or molecules that are much smaller in size compared to the wavelength of the incident light. In the context of Rayleigh thermometry, the scattering of light by gas molecules is used to infer the gas temperature.

The principle behind Rayleigh thermometry lies in the relationship between the scattering of light and the gas properties. The intensity of scattered light is directly proportional to the number of gas molecules and the area over which the scattering occurs. This means that an increase in either the number of particles or the gas volume will result in a higher scattered light intensity. [6]

However, the intensity of scattered light is inversely proportional to the temperature of the gas. As the gas temperature rises, the kinetic energy of the gas molecules increases, leading to more frequent collisions and changes in their positions. These changes cause fluctuations in the refractive index of the gas, which in turn affects the scattering of light. Consequently, an increase in gas temperature leads to a decrease in the intensity of scattered light.

By measuring the intensity of scattered light and knowing the gas volume, it is possible to determine the temperature of the combustion gases. The relationship between the scattered light intensity and temperature can be established through calibration using known temperature values. Once the calibration is performed, the intensity of scattered light can be used as an indicator of the gas temperature in real-time applications. (see figure 2.2)

Rayleigh thermometry has several advantages in the measurement of combustion gas temperature. It offers a non-intrusive and remote sensing method, allowing temperature measurements without physically contacting the gas. The application of conventional Rayleigh scattering in practical combustion systems is limited to

non-sooty flames due to significant interference caused by surfaces and particles. This interference poses one of the primary challenges associated with using this technique. [1]

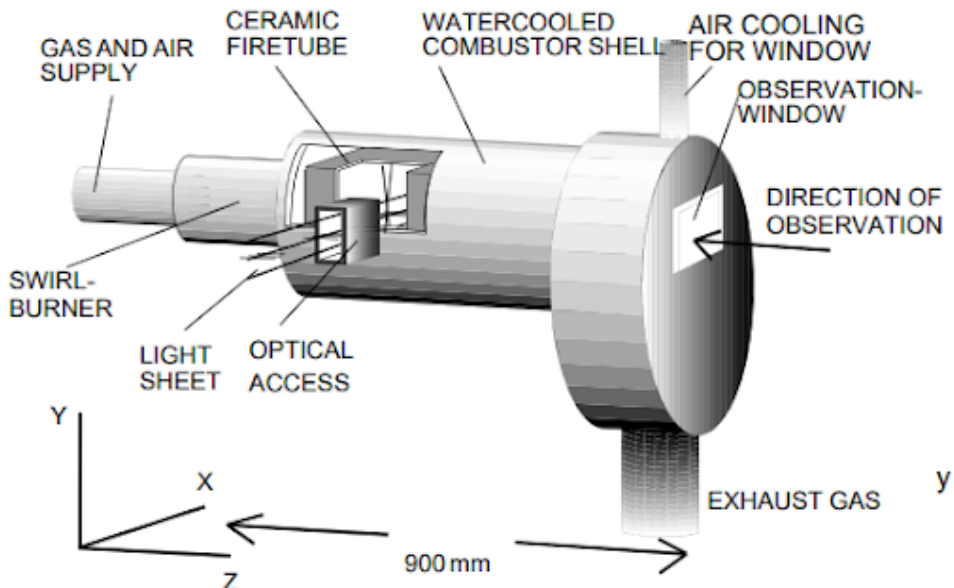


Figure 2.2: Rayleigh thermometry in combustor [7]

2.1.3 CARS

A nonlinear four-wave mixing procedure called coherent anti-Stokes Raman scattering (CARS) is employed to amplify the weak Raman signal. A Stokes laser beam and a pump laser beam interact in the CARS process to create an anti-Stokes signal at frequency $W_{CARS} = 2W_{pump} - W_{Stokes}$.[8]

CARS uses the principle of the anti-Stokes Raman effect. Unlike Raman spectrography, it uses many photons for the vibrations of the molecules thus producing a coherent output making it much stronger than the results from Raman spectroscopy. (see figure 2.3)

One of the main advantages of the system is its good accuracy in measuring data. It provides reliable and precise results, making it a valuable tool in various applications. However, there are several disadvantages associated with this system. Firstly, its

setup can be costly, requiring significant financial investment for installation and maintenance. Additionally, the system is highly sensitive, meaning that even slight variations in the environment or handling can affect its performance and accuracy. A newly developed rotational CARS technique can be used to improve the sensitivity. Moreover, it can only be used for single-point measurements, restricting its versatility compared to systems capable of capturing multiple points simultaneously.

Example of error: The C_2 radicals created when soot particles are burned by lasers are known to emit signals that interfere with the N_2 vibrational CARS signal's basic band. Large inaccuracies occur in areas with high soot volume fractions as a result of this interference, which grows with the number of soot particles present in a flame.

As the signals generated from both CARS and Rayleigh thermometry are comparatively weak, an intensified CCD (ICCD) camera is required for the detection. This increases the cost of the setup by manifolds. They are optimal for low-light or single photon applications due to the electron multiplying component of the intensifier.

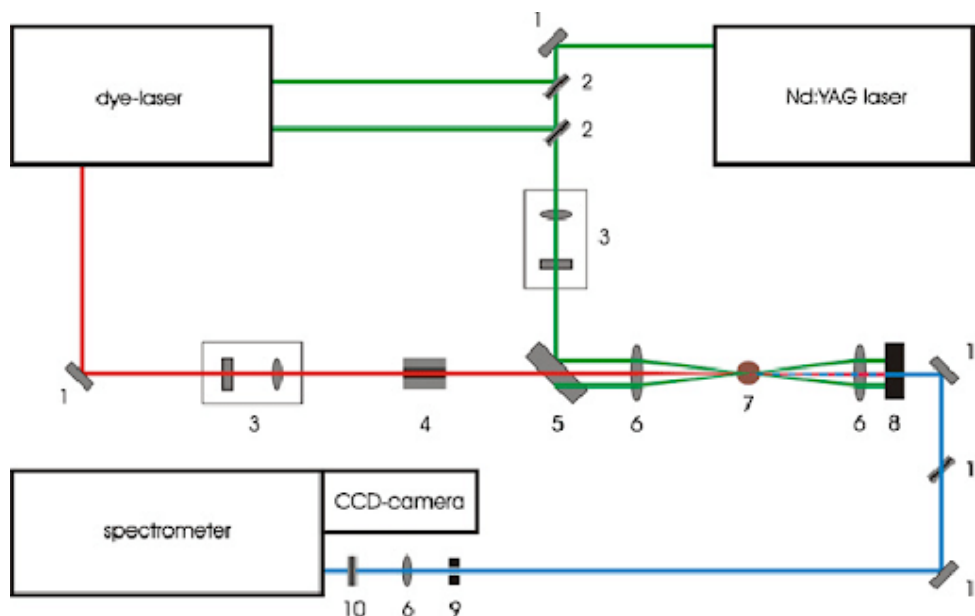


Figure 2.3: CARS technique [8]

2.1.4 Interferometry

Interferometric techniques are used for a wide range of applications from spectroscopy to gravitational wave detection. Michelson interferometer (see figure 2.4) is very popular in this type. It uses a beam splitter which divides the beam into two paths. The beam splitter can be half sliced mirror placed at 45 degrees to the incident beam. The two beams are then reflected back and superposed to get the interference pattern which is then detected by some device like a camera. Based on the application, modifications are made to the apparatus. To convert it for thermometry use, one or both mirrors are replaced by a thermalized sample. Replacing both mirrors increases the resolution. [9]

The system has the advantage of being based on a well-studied and proven device, which lends credibility to its functionality. However, it suffers from several disadvantages. Firstly, its accuracy is limited, making it unsuitable for applications that require precise measurements. Furthermore, there is a high scope of measurement errors, introducing uncertainty in the obtained data. The system is also sensitive to unknown variables, particularly temperature fluctuations, which can affect its performance. To address this, additional modeling, simulations, or experiments are necessary, increasing the complexity of its use. Moreover, incorrect alignment of the apparatus or vibrations can significantly impact its sensitivity. Lastly, the system is both expensive and bulky, adding to the overall cost and space requirements.

2.1.5 Infrared (IR) camera

This is very widely used for measuring the temperature of opaque objects. These are also called laser thermometers as they use a laser to point in the right direction. IR cameras use a lens to collect infrared radiation to a point and later convert it into an electrical output. Although it is made for opaque bodies like pan/ metals, it can be used to measure the flame temperature approximately using the CO₂ emission/absorption

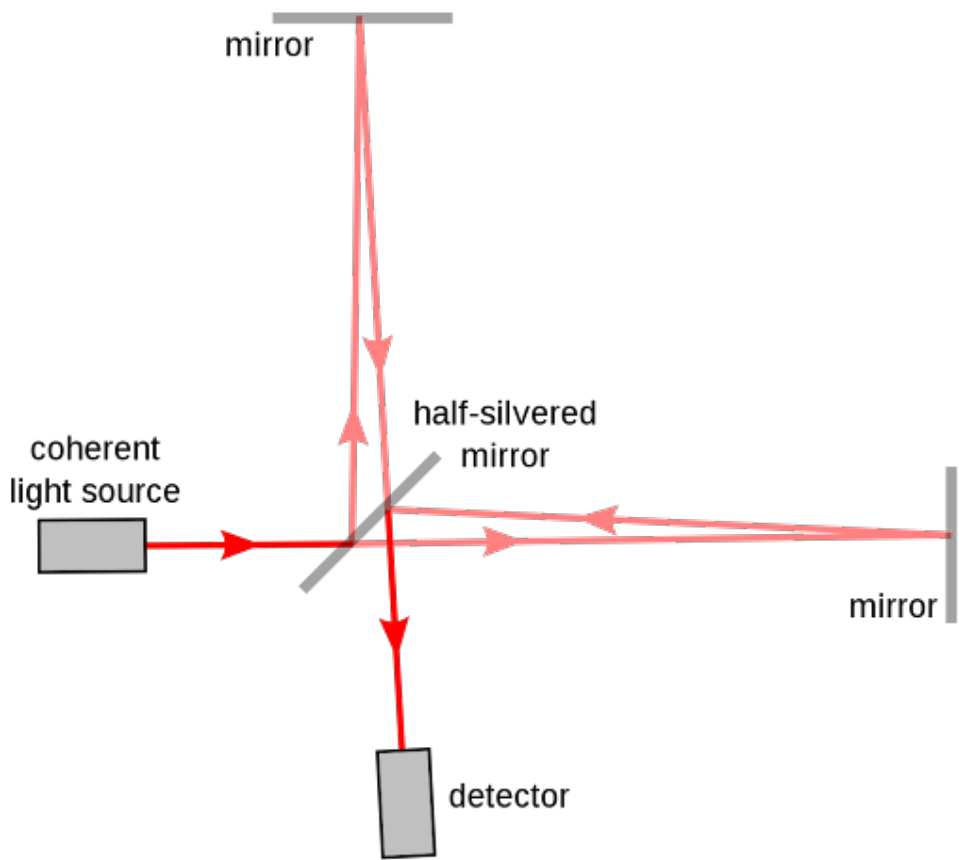


Figure 2.4: Michelson interferometer [10]

spectrum. The calculations become complex as the emissivity value can't be assumed constant for the complete flame the reason being a variation of the geometry of flame as well as the mole fraction CO_2 along the flame. These variations become more rapid in case of unsteady flames and hence IR cameras can only be used for steady flames.

One of the advantages of the system is its simple and inexpensive setup, making it accessible to a wide range of users. However, it has several notable disadvantages. Firstly, it cannot be used for unsteady flames, limiting its applicability in dynamic environments. Additionally, the system has very low accuracy, resulting in imprecise measurements. Complex calculations are required to obtain meaningful data, adding complexity to the process. Moreover, the system's measurements are unreliable, introducing uncertainty and reducing its overall usefulness.

2.1.6 Thin Filament Pyrometry

Thin filament pyrometry is a temperature measurement technique that involves the use of a silicon carbide filament placed within a flame. The radiation emitted by the filament is measured, and this radiation can be correlated to the temperature of the flame. (see figure 2.5)

The advantages of thin filament pyrometry are significant. Firstly, it allows for temperature measurements along a line within the flame, providing spatially resolved temperature data. This capability is particularly useful for understanding temperature distributions and variations within the flame, which can help optimize combustion processes. Another advantage is that thin filament pyrometry enables multi-point temperature measurements. By placing multiple filaments at different locations within the flame, simultaneous temperature measurements can be obtained, offering a comprehensive understanding of the thermal characteristics of the flame. Additionally, thin filament pyrometry is relatively simple and inexpensive to set up. The required equipment is generally affordable and readily available, making it accessible for various research and industrial applications.

The correlation between the radiation emitted by the filament and the actual temperature of the flame must be established through calibration experiments. This calibration process ensures accurate temperature measurements but requires additional equipment and time.

However, there are certain disadvantages associated with thin filament pyrometry. One significant drawback is the need for calibration using thermocouples. Furthermore, the presence of filaments within the flame can disturb the flow characteristics. The filaments can alter the flow patterns and affect the combustion process, potentially leading to inaccuracies in

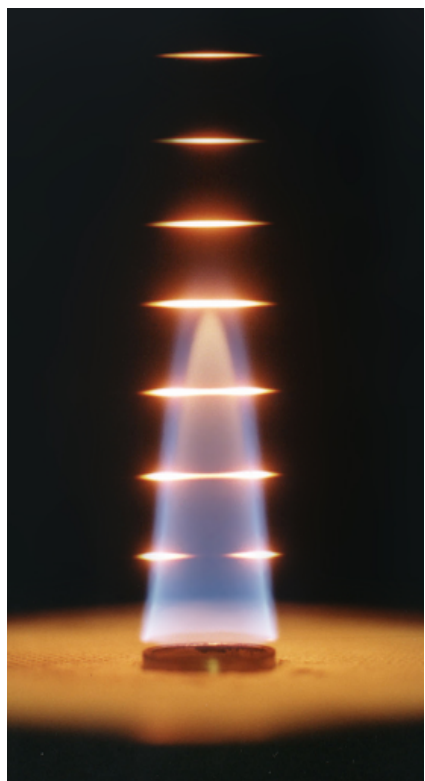


Figure 2.5: Thin filament pyrometry [11]

temperature measurements.

Lastly, the filaments used in thin filament pyrometry are fragile and susceptible to breakage over time. High temperatures, mechanical stresses, or chemical reactions within the flame can degrade the filaments, requiring regular replacement. This maintenance aspect should be considered when using this technique. [12]

2.1.7 Soot pyrometry

Most of the non-contact techniques discussed earlier had soot as the error generating factor. But, this technique uses soot itself to detect the temperature and hence it is very suitable for a sooty flame. A very common device used for this purpose is called a two-colour pyrometer. It uses thermal radiation at two different wavelengths to measure the temperature of the object.

2.2 Two-colour Pyrometry

Two-colour pyrometry is a narrow band soot pyrometry technique used to measure the temperature of objects by comparing the radiation intensities at two different wavelengths. It is a non-contact method that is widely employed in various industrial applications where accurate temperature measurement is crucial. [13]

2.2.1 Principle of Two-colour Pyrometry

The principle behind two-colour pyrometry is based on the relationship between the temperature of an object and the radiation it emits. According to Planck's law of blackbody radiation, the total power emitted by a blackbody is a function of its temperature and the wavelength of the emitted radiation. The relationship between

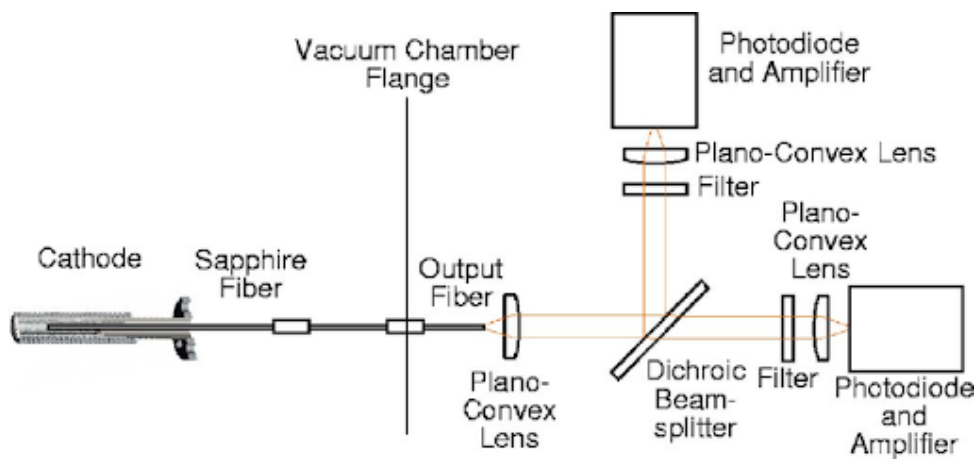


Figure 2.6: Two colour Pyrometry Setup [14]

the radiation intensity, temperature, and wavelength is given by the Stefan-Boltzmann law.

In two-colour pyrometry, two different wavelengths are selected, typically referred to as the short wavelength(λ_s) and long wavelength(λ_l). The ratio of the radiation intensities at these two wavelengths is then used to determine the temperature of the object. The selection of the two wavelengths is critical to ensure accurate temperature measurement, as it affects the sensitivity and accuracy of the technique. [15]

2.2.2 Implementation of Two-colour Pyrometry

To implement two-colour pyrometry, a pyrometer or an infrared radiation sensor is used. The sensor detects the radiation emitted by the object at the selected wavelengths. The detected radiation intensities are then converted into electrical signals, which are further processed to determine the temperature.

The calibration of the pyrometer is an essential step in two-colour pyrometry. It involves measuring the radiation intensities at the selected wavelengths for known temperatures. This calibration data is then used to establish a relationship between the measured radiation intensities and the corresponding temperatures. Typically, a calibration curve or equation is derived to convert the detected radiation intensities into temperature values.

2.2.3 Advantages of Two-colour Pyrometry

- Non-contact measurement: Two-colour pyrometry allows temperature measurement without physically touching the object, making it suitable for applications involving moving objects, hazardous materials, or objects at high temperatures.
- Wide temperature range: This technique can be used to measure temperatures ranging from a few hundred degrees Celsius to several thousand degrees Celsius.
- Accurate and reliable: By utilizing two wavelengths, two-colour pyrometry reduces the influence of factors such as emissivity variations, background radiation, and sensor response variations, leading to more accurate and reliable temperature measurements.
- Fast response time: Two-colour pyrometers can provide real-time temperature measurements, enabling quick monitoring and control of processes.

2.2.4 Hottel and Broughton Approach

It is an empirical emissivity model for radiating soot particles developed by Hottel and Broughton in 1932. [16]

According to this:

$$\varepsilon_\lambda(KL, \lambda) = 1 - e^{-\frac{KL}{\lambda^\alpha}} \quad (2.1)$$

$\varepsilon_\lambda(KL, \lambda)$ is the spectral emissivity, K is the absorption coefficient, L is the thickness of the flame along the line-of-sight (m), and KL, which can be treated as a whole called the optical thickness , and α is a constant, which depends on the physical and optical properties of soot in the flame. For a luminous flame, reasonable results can be obtained by assuming values of 4 for regions with nascent soot, and 1.38 for the regions laden with matured soot particles.

KL and T are the only unknown parameters in the following modified expression of Planck's Law.

$$I_\lambda(T, \lambda) = \frac{1}{\pi} \left(1 - e^{-\frac{KL}{\lambda^\alpha}}\right) \frac{C_1}{\lambda^5} \frac{1}{e^{\frac{C_2}{\lambda T}} - 1} \quad (2.2)$$

It can then be solved for T when the two intensities are known for the two wavelengths λ_1 and λ_2 . [17]

2.2.5 Comparison with colour-ratio pyrometry

Two-colour pyrometry and colour ratio pyrometry are two different techniques used for temperature measurement based on the analysis of thermal radiation. While both methods involve the comparison of radiation intensities, there are some key differences between them.

Two-colour pyrometry, as discussed earlier, measures the temperature of an object by comparing the radiation intensities at two different wavelengths. The ratio of intensities at the selected wavelengths is used to determine the temperature. This technique requires careful wavelength selection and calibration to establish a relationship between intensity ratio and temperature. Two-colour pyrometry is commonly used in industrial applications and offers accurate and reliable temperature measurements across a wide range.

Colour ratio pyrometry, on the other hand, involves the analysis of colour or spectral characteristics of the thermal radiation emitted by an object. Instead of comparing radiation intensities at specific wavelengths, this method examines the ratio of intensities at two different regions of the electromagnetic spectrum. The colour ratio is determined by dividing the intensity in one spectral band (usually a shorter wavelength range) by the intensity in another spectral band (usually a longer wavelength range). This colour ratio is then correlated with the object's temperature using calibration data. [18]

The key distinction between the two techniques lies in the basis of their temperature determination. Two-colour pyrometry focuses on the comparison of radiation intensities at specific wavelengths, while colour ratio pyrometry examines the spectral composition and ratio of intensities in different wavelength regions.

Both techniques have their advantages and limitations. Two-colour pyrometry provides accurate temperature measurements, compensating for variations in emissivity, while colour ratio pyrometry can be more versatile in terms of spectral band selection. The choice between the two methods depends on the specific requirements of the application and the available spectral information.

2.3 Colour Ratio Pyrometry

The electrons and protons inside the matter are continuously moving and generating heat. When this heat gets converted into EM radiation, it is called thermal radiation. Every object above the absolute zero temperature emits thermal radiation. Most of the radiation at room temperature is in the IR range, hence not visible to the naked eye.

The wavelength of the light emitted depends on the object's temperature. Wiens law states that the wavelength of maximum emission of a black body is inversely proportional to its temperature. (see figure 2.7)

The intensity of the light (thermal radiations) emitted by the soot particle can more accurately be given by Planck's formula: (formulated by German physicist Max Planck in 1900)

$$I(\lambda, T) = \varepsilon(\lambda) \frac{2\pi hc^2}{\lambda^5 (e^{\frac{hc}{\lambda k_B T}} - 1)} \quad (2.3)$$

*The meaning of the symbols can be found under nomenclature.

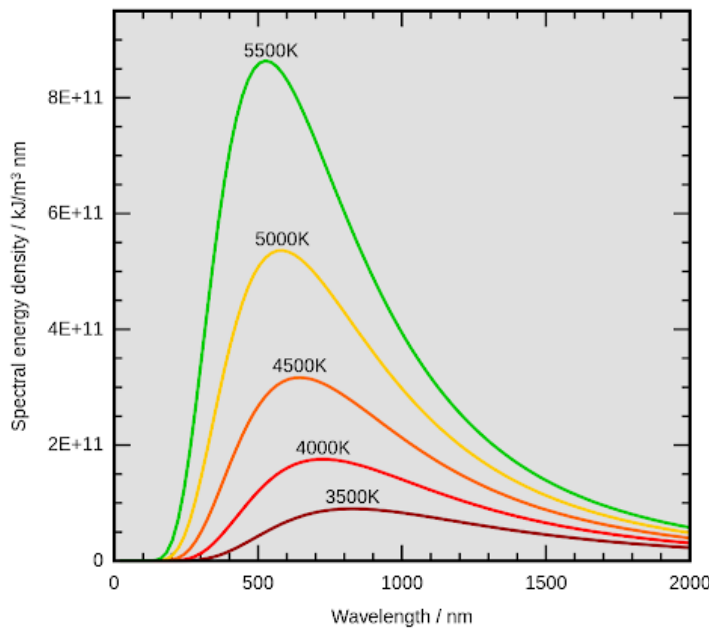


Figure 2.7: Wien's displacement law(formulated by German physicist Wilhelm Wien in 1893) [19]

The camera acts as a broad band optical sensor.[20] [21] When measured by a camera, the signal detected on a pixel can be calculated as:

$$S_F = 2\pi hc^2 \tau \int_{\lambda_1}^{\lambda_2} \frac{\varepsilon(\lambda)\eta(\lambda)}{\lambda^5(\exp(hc/\lambda k_B T) - 1)} d\lambda \quad (2.4)$$

The limits of integration are usually the end wavelengths of the visible spectrum (400 and 700 nm)

Once the image is processed and RGB values of all the pixels are obtained, we start normalizing the values, first on the arbitrary scale and then to the scale of 0 to 1. First, we choose R. We convert all R values to an arbitrary scale using the following formula:

$$\eta_{R_arb}(\lambda) = \frac{R}{P\tau} \quad (2.5)$$

After this, they are normalized to the scale of 0 to 1.

$$\eta_{R_scaled}(\lambda) = \frac{\eta_{R_arb}}{MAX(\eta_{R_arb})} \quad (2.6)$$

And similarly for B and G values:

$$\eta_{B_scaled}(\lambda) = \frac{\eta_{B_arb}}{\frac{R}{B}} \quad (2.7)$$

$$\eta_{G_scaled}(\lambda) = \frac{\eta_{R_scaled}}{\frac{R}{G}} \quad (2.8)$$

A further normalization can be done so that all three values come on one scale. [1]

These normalized signal values, when plotted against wavelengths are called spectral response curve. It is the identity of a particular camera sensor. These spectral response curves can further be used to find theoretical lookup curves that are plots of colour ratios against temperature. These lookup curves can later be used to find temperature from a new flame image.

Chapter 3

Imaging Technology

3.1 Camera sensors

3.1.1 CCD (Charge-Coupled Device)

CCD is a type of image sensor technology widely used in digital cameras and video cameras. It consists of an array of light-sensitive elements called pixels that convert incoming light into an electrical charge.

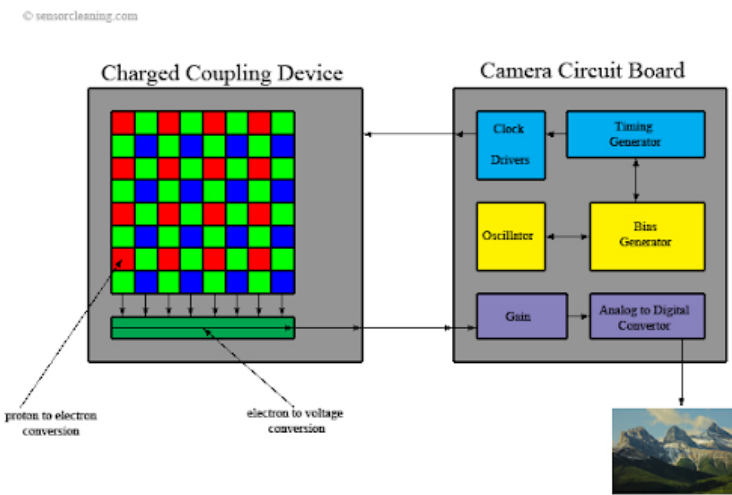


Figure 3.1: CCD camera sensor [22]

3.1.1.1 History of CCD

Initially, CCDs were primarily used in scientific and astronomical applications due to their high sensitivity and low noise characteristics. They were used in early digital imaging devices, such as scanners and early digital cameras.

In the late 1990s and early 2000s, CCD sensors gained popularity in consumer digital cameras, offering higher image quality compared to other image sensor technologies of that time. However, with advancements in CMOS technology and its advantages in terms of power consumption, readout speed, and integration of circuitry, CCD sensors started to decline in popularity in the consumer market. Today, CCD sensors are mainly used in specialized applications, such as scientific imaging, astronomy, and high-end professional photography.

3.1.1.2 The key features of CCD

- **Pixel Structure:** CCD sensors have a complex structure where each pixel consists of a photosensitive element and a charge storage element. The incoming photons generate electrons in the photosensitive element, which are then transferred to the storage element. (see figure 3.1)

- **Analog Signal Processing:** CCD sensors utilize analog signal processing techniques to convert the stored charge into an analog voltage. This voltage is then amplified and converted into a digital signal through an analog-to-digital converter.
- **High Image Quality:** CCD sensors are known for their excellent image quality, especially in terms of colour accuracy, dynamic range, and low noise levels. They are commonly used in applications where high-quality images are critical, such as professional photography and scientific imaging.
- **Slow Readout Speed:** One limitation of CCD sensors is their relatively slow readout speed. Each pixel's charge must be sequentially read, which can result in slower continuous shooting speeds and video frame rates compared to CMOS sensors.

3.1.2 CMOS (Complementary Metal-Oxide-Semiconductor)

CMOS is another type of image sensor technology that has gained popularity in recent years due to its advantages over CCD. Unlike CCD, CMOS sensors integrate both the image sensor and image processing circuitry on the same chip.

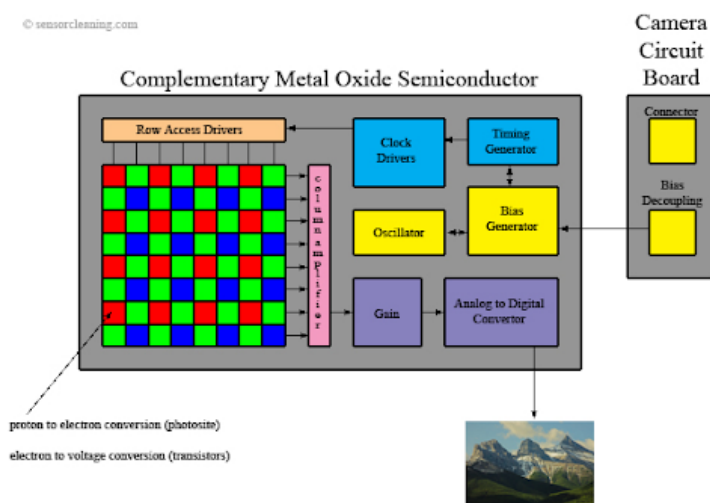


Figure 3.2: CMOS camera sensor [22]

3.1.2.1 History of CMOS

Initially, CMOS technology found applications in digital logic circuits, microprocessors, and memory chips. It was not widely considered for image sensor applications due to limitations in performance and image quality.

In the late 1990s and early 2000s, significant advancements were made in CMOS image sensor technology. The integration of amplifiers, digitization circuitry, and other signal processing components on the same chip improved readout speed, noise performance, and power efficiency. With these advancements, CMOS sensors started gaining popularity in consumer electronics, particularly in smartphones and digital cameras, due to their lower power consumption, faster readout speeds, and the ability to integrate additional functionalities on the sensor chip.

3.1.2.2 The key features of CMOS

- **Pixel Structure:** CMOS sensors have a simpler pixel structure compared to CCD, with each pixel having its own amplifier and digitization circuitry. This enables parallel readout of each pixel's charge, resulting in faster readout speeds. (see figure 3.2)
- **Digital Signal Processing:** CMOS sensors perform analog-to-digital conversion at each pixel, allowing them to directly output digital signals. This eliminates the need for additional external circuitry and simplifies the overall system design.
- **Lower Power Consumption:** CMOS sensors generally consume less power than CCD sensors due to their ability to selectively activate specific pixels for readout. This makes CMOS sensors suitable for portable devices like smartphones and digital cameras.
- **Rolling Shutter Effect:** CMOS sensors employ a rolling shutter mechanism, where each row of pixels is exposed and read out sequentially. This can introduce a distortion known as the rolling shutter effect, which can cause image skewing or artifacts in fast-moving scenes.

- Advancements in Technology: CMOS sensors have seen significant technological advancements, leading to improvements in image quality, dynamic range, and noise performance. They have become the dominant sensor technology in many consumer devices due to their versatility and cost-effectiveness. [23] [24]

3.2 Bayer Filter

The Bayer filter is a colour filter array (CFA) that is widely used in most digital cameras and image sensors.

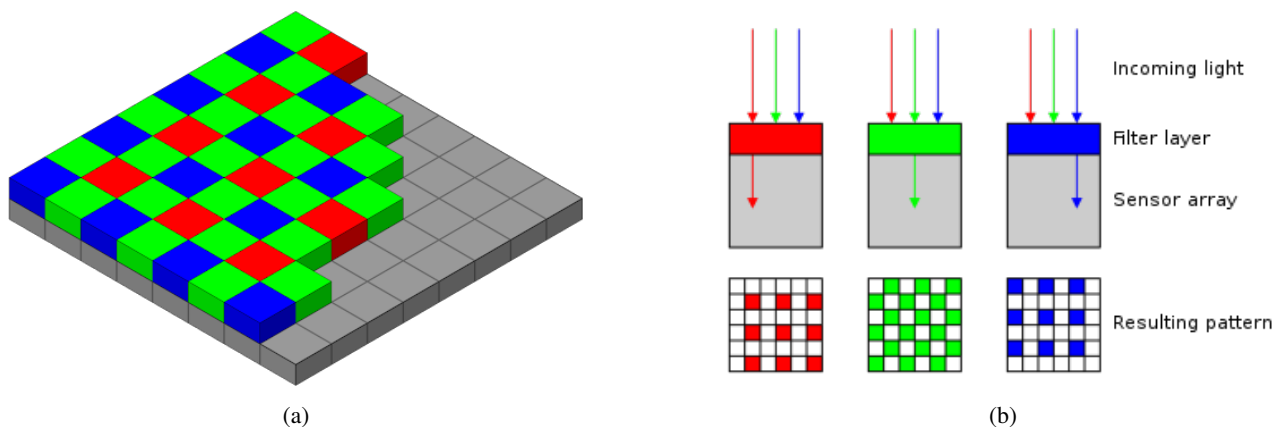


Figure 3.3: Bayer Filter [25]

3.2.1 The Purpose of the Bayer Filter

The primary purpose of the Bayer filter is to capture colour information by selectively filtering light into separate red, green, and blue (RGB) colour channels. The filter is placed on top of the image sensor, which consists of millions of light-sensitive photosites (pixels).

3.2.2 Bayer Filter Pattern

The Bayer filter pattern is a mosaic of red, green, and blue colour filters arranged in a specific pattern. The most common pattern is a 2x2 repeating arrangement of red, green, green, and blue filters in a checkerboard pattern. This pattern is also referred to as the RGGB Bayer filter pattern. (see figure 3.3)

In this pattern, the red filter allows only red light to pass through to the corresponding pixel. The blue filter allows only blue light to pass through to the corresponding pixel. The green filters allow green light to pass through to the corresponding pixels. The green filters are twice as many as the red and blue filters because the human eye is more sensitive to green light, and having more green samples helps improve the overall image quality and colour accuracy. [25]

3.2.3 Colour Reconstruction

As each pixel in the Bayer filter can only capture a single colour, the missing colour information needs to be interpolated or reconstructed to produce a full-colour image. This process is known as demosaicing or colour interpolation.

Demosaicing algorithms analyze the surrounding pixels with different colour information to estimate the missing colour values. Various interpolation techniques, such as bilinear interpolation, nearest-neighbor interpolation, and more sophisticated algorithms like adaptive filtering or edge-directed interpolation, are used to reconstruct the full-colour image.

3.2.4 Challenges and Limitations

The Bayer filter introduces several challenges and limitations in colour imaging:

- colour Artifacts: Since each pixel captures only one colour, the demosaicing process can introduce colour artifacts like colour fringing or false colours along high-contrast edges.
- Spatial Resolution: The Bayer filter reduces the effective spatial resolution of the image sensor, as only one colour sample is available for each pixel location.
- Sensitivity to Noise: The demosaicing process can amplify noise, resulting in a loss of image quality, particularly in low-light conditions.
- Limited colour Accuracy: The Bayer filter cannot capture all colours simultaneously, leading to potential inaccuracies in colour reproduction, especially for fine colour details and subtle colour transitions.

3.2.5 Alternative Colour Filter Arrays

There are alternative colour filter arrays that aim to overcome some of the limitations of the Bayer filter, such as the X-Trans filter [26] used in some Fujifilm cameras. These alternative patterns employ different arrangements of colour filters, which can offer improved colour reproduction, reduced colour artifacts, and higher effective resolution.

3.3 Threshold Levels

3.3.1 Black Level

The black level refers to the signal value or voltage level that corresponds to the absence of light hitting the camera sensor. It represents the darkest part of the image, where there should be no light or minimal light present. The black level is crucial for accurately determining the noise level in an image. By measuring the signal level when no light is present, it provides a reference point for distinguishing between actual image data and sensor noise.

Camera manufacturers calibrate the black level during the sensor manufacturing process to ensure consistent performance across sensors. However, in some cases, black level calibration may need to be adjusted or corrected, especially in high-end cameras or professional workflows.

3.3.2 White Level

The white level represents the signal value or voltage level that corresponds to the maximum light intensity that the camera sensor can capture without saturating. It represents the brightest part of the image, such as highlights or bright light sources. The white level is crucial for proper exposure determination. By knowing the sensor's maximum capability to capture light, photographers can adjust the exposure settings to avoid overexposure or clipping of highlights.

The white level is typically calibrated during the camera manufacturing process to ensure consistent performance. However, like the black level, adjustments or corrections may be necessary in certain situations.

3.4 DSLR Camera

3.4.1 History of DSLR Cameras

The development of DSLR cameras can be traced back to the early days of film SLR (Single-Lens Reflex) cameras. The transition from film to digital imaging brought significant advancements, resulting in the introduction of digital SLR cameras in the late 1990s and early 2000s.

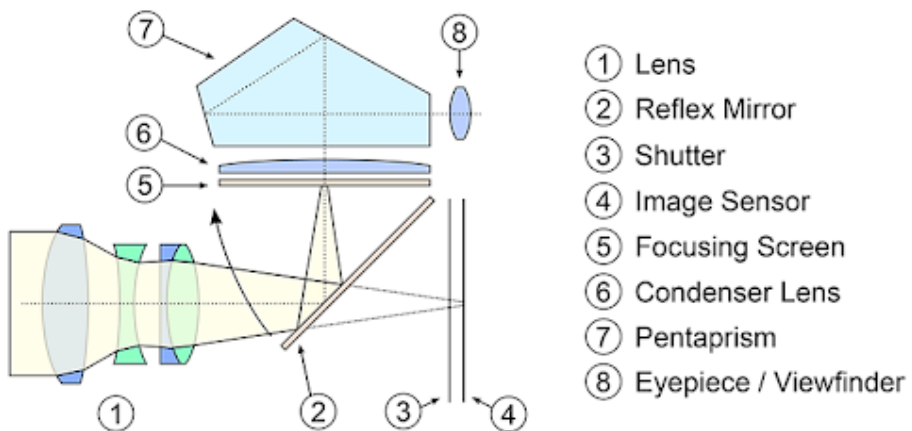


Figure 3.4: DSLR Camera schematic [27]

3.4.2 Current Technology of DSLR Cameras

Here are some key aspects of current DSLR camera technology [27]:

- **Optical Viewfinder and Mirror Mechanism:** One defining feature of DSLR cameras is the presence of an optical viewfinder (OVF) and a mirror mechanism. The mirror reflects the light entering the lens upwards into the OVF, allowing the photographer to see the scene directly through the lens. When the shutter is released, the mirror quickly moves out of the way to expose the camera's image sensor. (see figure 3.4)
- **Image Sensor:** DSLR cameras feature larger image sensors compared to most compact cameras or smartphones. Common sensor sizes include APS-C (Advanced Photo System type-C) and full-frame (equivalent to the traditional 35mm film size). The larger sensor size provides advantages such as better low-light performance, improved dynamic range, and enhanced control over depth of field.
- **Manual Controls and Customization:** DSLR cameras provide extensive manual control over various settings, giving photographers precise control over exposure, shutter speed, aperture, ISO, and other parameters. These cameras often feature dedicated dials and buttons for quick adjustments, allowing photographers to customize their shooting experience based on their preferences and shooting style.

3.5 Phone Camera Sensors



Figure 3.5: Phone camera sensor [28]

3.5.1 History of Phone Camera Sensors

The integration of cameras into mobile phones at the end of the 20th century marked a significant shift in the way we capture and share images. Early mobile phone cameras utilized low-resolution sensors, typically around 0.1 to 1 megapixel (MP), primarily for basic snapshots. As technology advanced, phone cameras evolved to higher resolutions, improved image quality, and additional features. Manufacturers began incorporating more capable image sensors, often adapted from digital camera technologies, to enhance the photographic capabilities of mobile devices.

3.5.2 Current Technology of Phone Camera Sensors

Here are some key aspects of current phone camera sensor technology:

- **Sensor Types:** Phone camera sensors primarily fall into two categories: CCD (Charge-Coupled Device) and CMOS (Complementary Metal-Oxide-Semiconductor).

CMOS sensors have become more prevalent due to their lower power consumption, faster readout speeds, and integration capabilities.

- Resolution: Phone camera sensors now offer resolutions ranging from 12 MP to 108 MP and beyond. Higher megapixel counts allow for more detailed images, enabling users to crop or zoom in without significant loss in quality. However, megapixel count alone does not determine image quality; other factors such as pixel size, sensor size, and image processing algorithms also play crucial roles.
- Pixel Size: Pixel size refers to the physical dimensions of individual pixels on the sensor. Larger pixel sizes tend to capture more light, leading to improved low-light performance and better overall image quality. Phone camera sensors today strike a balance between higher pixel counts and larger pixel sizes to optimize image quality in various lighting conditions.
- Sensor Size: Sensor size plays a vital role in image quality, especially in low-light environments and depth of field control. While phone camera sensors are inherently smaller than those found in dedicated cameras, manufacturers have made efforts to increase sensor sizes within the space constraints of mobile devices. Some phones now feature sensors with larger physical dimensions, such as 1/1.3" or even 1" in diagonal size, delivering improved low-light sensitivity and dynamic range.
- Multi-Camera Systems: Many modern smartphones feature multiple camera sensors, each with different focal lengths or specialized functions. This allows for versatile photography capabilities, including optical zoom, ultra-wide-angle shots, macro photography, and depth sensing for portrait effects. (see figure 3.5)

3.6 Parameters in cameras

3.6.1 ISO

ISO refers to the sensitivity of the camera sensor to light. It is derived from the ISO film speed standards used in traditional film photography. In digital cameras, ISO can

be adjusted to control the camera's sensitivity to light. Higher ISO values (e.g., ISO 800, ISO 1600) make the sensor more sensitive, allowing for better performance in low-light situations but may introduce more digital noise or grain in the image. Lower ISO values (e.g., ISO 100, ISO 200) result in less noise but require more light for proper exposure.

3.6.2 Shutter Speed

Shutter speed determines the duration for which the camera's shutter remains open, allowing light to reach the image sensor. It is measured in seconds or fractions of a second. Fast shutter speeds (e.g., 1/1000s) freeze motion and are suitable for capturing fast-moving subjects, while slow shutter speeds (e.g., 1/4s) create motion blur effects or capture long-exposure shots. Shutter speed also affects the amount of light entering the camera, with longer exposures allowing more light and shorter exposures reducing the amount of light.

3.6.3 Aperture

Aperture refers to the opening of the camera's lens through which light passes. It is measured in f-stops, denoted by numbers such as f/2.8, f/5.6, etc. Aperture controls the amount of light reaching the camera sensor and also influences the depth of field. A wider aperture (smaller f-number) lets in more light and results in a shallower depth of field, with the subject in focus and the background blurred. A narrower aperture (larger f-number) reduces the amount of light and increases the depth of field, bringing more of the scene into focus.

3.6.4 White Balance

White balance refers to the adjustment of the camera's colour response to ensure accurate colour reproduction under different lighting conditions. Different light sources have varying colour temperatures, which can result in colour casts in images. White balance allows to compensate for these colour temperature differences and produce more natural-looking colours. Common white balance settings include Auto, Daylight, Cloudy, Shade, Tungsten, Fluorescent, and Custom. Some cameras also provide the option to fine-tune white balance manually.

3.6.5 Focus Modes

Focus modes determine how the camera focuses on the subject. Common focus modes include [29]:

- Single Autofocus (AF-S): The camera focuses on the subject when the shutter button is half-pressed, and locks the focus until the image is captured.
- Continuous Autofocus (AF-C): The camera continuously adjusts the focus as the subject or the camera moves. It is useful for capturing moving subjects, such as sports or wildlife photography.
- Manual Focus (MF): The photographer manually adjusts the focus ring on the lens to achieve the desired focus. This mode provides complete control over the focus but requires manual adjustment.
- Automatic Autofocus (AF-A): The camera automatically switches between single autofocus (AF-S) and continuous autofocus (AF-C) based on the subject's movement. It is suitable for situations where the subject's motion may vary.

3.7 Image File Format

Digital cameras, including DSLRs and phone cameras, provide options for saving images in different file formats. The most common formats include:

3.7.1 JPEG

A compressed file format that is widely supported and suitable for everyday photography. JPEG files are smaller in size but may sacrifice some image quality due to compression.

3.7.2 RAW

A lossless file format that preserves all the sensor data and offers maximum flexibility for post-processing. RAW files contain more information and allow for greater control over settings like white balance and exposure during editing.

3.7.3 TIFF

A lossless file format that maintains image quality but results in larger file sizes compared to JPEG. TIFF files are often used in professional workflows or when maximum image quality is required.

3.7.4 DNG

DNG (Digital Negative) is an open, non-proprietary RAW file format that retains the original sensor data, providing maximum flexibility for post-processing and preserving image quality.

3.8 Camera APIs(Application programming interface)

To unlock the full potential of smartphone cameras, camera APIs (Application Programming Interfaces) play a crucial role. An API (Application Programming Interface) is a set of rules and tools that enables software applications to communicate and interact with each other. It acts as a bridge, allowing different systems to exchange information and access functionality without needing to understand the underlying details. APIs are essential for integrating services, building reusable components, and enabling interoperability between software systems. They provide standardized ways for developers to access and utilize the capabilities of existing applications or services.

3.8.1 CameraAPI

CameraAPI is an earlier version of the camera interface introduced in Android. It provides a straightforward and easy-to-use framework for accessing and controlling camera functionalities on Android devices. CameraAPI offers basic camera controls, including image capture, exposure adjustments, and focus modes. However, its capabilities are limited compared to the newer CameraAPI2.

3.8.2 CameraAPI2

CameraAPI2 is an enhanced and more versatile camera API introduced in Android version 5.0 (Lollipop). It builds upon the foundation of CameraAPI and provides a comprehensive set of features and controls, offering developers greater flexibility and fine-grained control over the camera hardware. CameraAPI2 supports advanced functionalities such as manual focus, exposure control, and RAW image capture, making it a preferred choice for developers seeking professional-grade camera capabilities. [30] [31]

3.8.3 Comparison

- **RAW Image Capabilities:** One of the significant differences between CameraAPI and CameraAPI2 lies in their support for RAW image capture. RAW images contain unprocessed and uncompressed sensor data, allowing for greater post-processing flexibility and image quality enhancements. CameraAPI2 introduced robust RAW image support, enabling developers to capture RAW images directly from the camera sensor. This feature provides photographers and image editing enthusiasts with the ability to extract the maximum amount of information from the captured images. On the other hand, CameraAPI lacks native RAW image support, limiting the post-processing possibilities and overall image quality.
- **Rollout Timeline:** CameraAPI was initially introduced with Android version 1.0 and served as the primary camera API for Android devices until the release of CameraAPI2. Its rollout timeline closely aligns with the early stages of Android's development, as it was the default camera interface for several Android versions. CameraAPI2 made its debut with Android version 5.0 (Lollipop). While it was introduced as an upgrade to CameraAPI, its adoption took some time due to device manufacturers needing to update their firmware and support the new API. However, over time, CameraAPI2 gained widespread acceptance and became the recommended choice for developers seeking advanced camera capabilities on Android devices.

3.9 Importance of RAW format

In colour ratio pyrometry, the RAW format is important because it allows for capturing and processing unprocessed sensor data from a digital camera without any in-camera adjustments or modifications. RAW format preserves the full range of data captured by the camera sensor, including the raw red, green, and blue (RGB) colour values.

The importance of RAW format in colour ratio pyrometry lies in its ability to provide linear and accurate colour information. Linearity refers to the direct relationship

between the actual intensity of light hitting the camera sensor and the recorded pixel values. In other words, if the light intensity doubles, the pixel values should also double. To obtain accurate temperature measurements, it is important to have a linear response from the camera sensor. If the camera's response is non-linear, it can introduce errors in the colour ratio calculations, leading to inaccurate temperature estimations. This is where the RAW format comes into play.

RAW format allows for direct access to the unprocessed sensor data, which means that the camera's internal algorithms for adjusting white balance, exposure, gamma correction, and other image processing parameters are bypassed. This enables a more accurate representation of the sensor's response to light, preserving the linearity of the data.

By using RAW format in colour ratio pyrometry, it is possible to minimize the impact of any non-linearities caused by in-camera processing. This ensures that the captured colour ratios correspond more closely to the actual temperature of the observed object, improving the accuracy of temperature measurements.

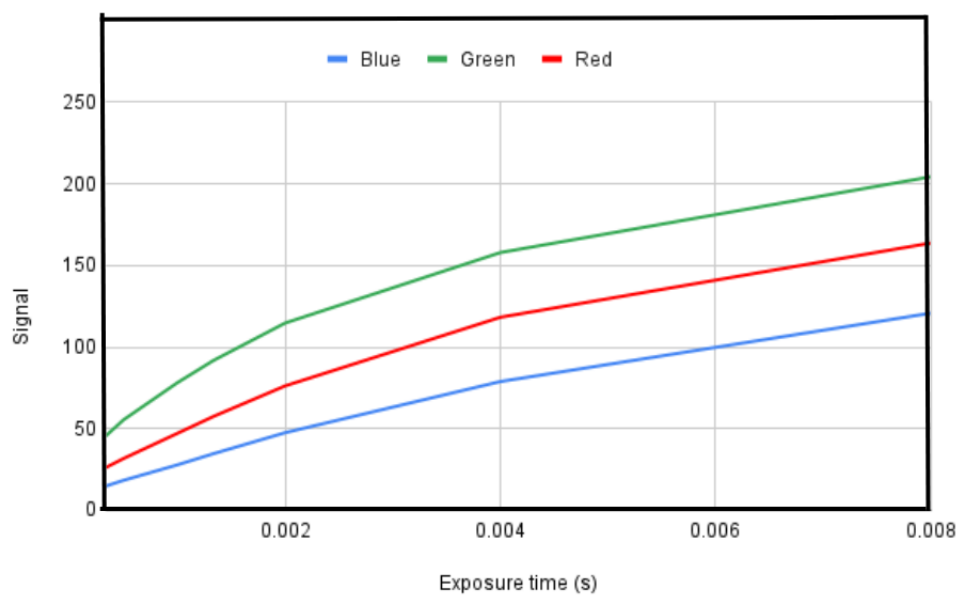


Figure 3.6: Non linearity in exposure time if JPG images are used instead of raw images

Processing RAW data requires specialized software capable of interpreting and converting the raw sensor data into a viewable image. However, for colour ratio pyrometry, the raw data is usually processed and analyzed directly without being converted into

a viewable image, as the objective is to extract temperature information rather than creating a visual representation. The graph below (see figure 3.9) shows the average values of R, G and B pixels for JPEG images of the same picture with different exposure times.

3.10 Sensors used in this study

To validate the CRP method developed, the following devices and corresponding sensors were used in this study. Sony and Samsung are the only two major players when it comes to smartphone camera sensors. So, these devices cover a major spectrum of the available sensors.

Table 3.1: Sensors used in the study

| Number | Device | Sensor | Specifications |
|--------|-------------------------------|--------------------|---------------------------------------|
| 1 | One Plus 9RT 5G | Sony IMX766 | 50 MP resolution 1.67" image sensor |
| 2 | Realme X3 Super-zoom | Samsung GW1 sensor | 64 MP resolution 1/1.72" image sensor |
| 3 | Motorola Moto G82 | Samsung S5KJN1 | 50 MP resolution 1/2.76" image sensor |
| 4 | Raspberry Pi Camera Module V2 | Sony IMX708 | 12 MP resolution 1/1.3" image sensor |

Chapter 4

Experimental Setups

In this chapter, we will look into various setups used for the experimental work related to the research work. After developing the procedures for CRP, the method and the product was validated by doing different experiments.

4.1 Monochromator setup

The sensors used for CRP need to be calibrated first in order to obtain the temperature versus colour ratio data. The first step of this calibration is flashing monochromatic wavelength light on the sensor and getting the raw readings of the pixel values to get

the variation in R, G and B with wavelength.

4.1.1 Monochromator

A monochromator is a scientific instrument used to isolate and select a specific wavelength of light from a broader range of wavelengths. It is commonly used in various fields such as spectroscopy, optics, and analytical chemistry. The HOLMARC Spectra Quasar Series Monochromator, HO-SP-SQR200F used in the experiment utilizes a single grating. (see figure 4.1)

The angular position of the grating within a monochromator is crucial in determining which wavelengths are transmitted through the exit slit. By employing a sine drive mechanism, the monochromator can precisely adjust the angle of the grating to selectively transmit a specific wavelength of light. This adjustment can be done without altering the positions of mirrors and slits, which ensures the stability and alignment of the instrument. [32]

Monochromators are used in numerous applications, including spectroscopy, fluorescence analysis, absorption and transmission measurements, and colourimetry. They are employed in scientific research, quality control processes, and industrial applications where precise control of light wavelengths is necessary.

4.1.2 Power meter

An optical power meter is a device used to measure the power or intensity of an optical signal. It plays a crucial role in the field of optics and photonics, providing accurate measurements of light power levels in various applications such as fiber optic communication systems, laser testing, and optical component characterization.



Figure 4.1: HO-SP-SQR200F monochromator [33]

The primary function of an optical power meter is to determine the power of an optical signal in terms of watts. It consists of a photodetector or a sensor that converts the incoming light energy into an electrical current, followed by a display unit that presents the power measurement in the desired format. [34]

The Holmarc HO-OPM-01UV optical power meter (see figure 4.2) used has a Silicon photodiode and has an active area of 5.8 mm x 5.8 mm to measure the optical power of a light beam.



Figure 4.2: HO-OPM-01UV optical power meter [35]

4.1.3 Sensor Calibration

The phone camera sensors mentioned in Chapter 3 were calibrated on the monochromator to get the spectral response curves. Along with phone camera sensors, raspberry pi camera module v2 was also calibrated.

The spectral response curves of phone camera sensors describe how sensitive the sensors are to different wavelengths of light. These curves provide information about the sensor's ability to capture and reproduce colours accurately. The exact spectral response curves vary depending on the specific camera sensor used in a phone, as different manufacturers may employ different technologies and designs.

Typically, phone camera sensors are designed to prioritize capturing light within the visible light spectrum, which ranges from approximately 400 to 700 nm. Manufacturers often do not disclose the exact spectral response curves of their camera sensors in detail. Instead, they may provide general information about the sensor's capabilities, such as its pixel size, pixel binning technology, or low-light performance.

The procedure for calibration is as follows:

1. The sensor is fixed at a particular distance from the monochromator exit. The distance from the monochromator doesn't affect the results. [2]
2. The monochromator wavelength is varied using the controller in the interval of 10nm and the raw image is captured.
3. The image is post-processed using the MATLAB code (see Appendix A), where the raw data is first divided into R, G and B matrices without demosaicing.
4. A particular area full of light from the monochromator is cropped and the averages of non-zero elements (50% numbers in G matrix, and 75% each in R and B matrix are 0 because of non-demosaicing) are taken for R, G and B matrices respectively. These are signals, as mentioned in Chapter 2.

5. Once all the readings for visible spectral band are taken (400 nm to 700 nm), the power meter data is obtained by replacing the sensor with the optical power meter and repeating the procedure.
6. The signals are normalized as mentioned in Chapter 2 and plotted as spectral response curves.

The older procedure involved Neutral Density filters (ND filters) to reduce the intensity of the monochromator to remove saturation in the image. As mentioned in Chapter 3, the saturation of the pixel is when the pixel value reaches the white level. Saturation causes major problems to the CRP procedure as the saturated value is not the true value of the pixel. These filters are designed to reduce the amount of light entering the camera's lens without affecting the colour or hue of the image. ND filters are commonly used in various situations where controlling the amount of light is crucial to achieving the desired creative effects.

The primary purpose of an ND filter is to extend the exposure time, allowing for longer shutter speeds even in bright conditions. By reducing the intensity of light reaching the camera's sensor, ND filters enable photographers to capture motion blur or create stunning long-exposure images. This is especially useful in situations where there is too much ambient light or when working with moving subjects, such as waterfalls, rivers, or bustling city streets.

The OD (Optical Density) of an ND filter refers to its light-blocking capacity or the amount of light it can reduce. It is a measure of the filter's ability to attenuate or block incoming light. The higher the OD value, the greater the light reduction provided by the filter. There are various types of ND filters, like absorptive, reflective or variable ND filters. In the experiments, Holmarc's absorptive ND filters of OD 2 and 3 were used.

Eventually, the problem with the ND filter was identified. When the power meter data was recorded with and without ND filter, it was found that the transmittance of the ND filter is wavelength dependent. (see figure 4.3) Though they are called as ND

filters, the light of all wavelengths is not transmitted uniformly through the ND filter. Because of this, the calibration had errors. Hence, ND filters were discarded and the problem of saturation was corrected by reducing the aperture of the monochromator.

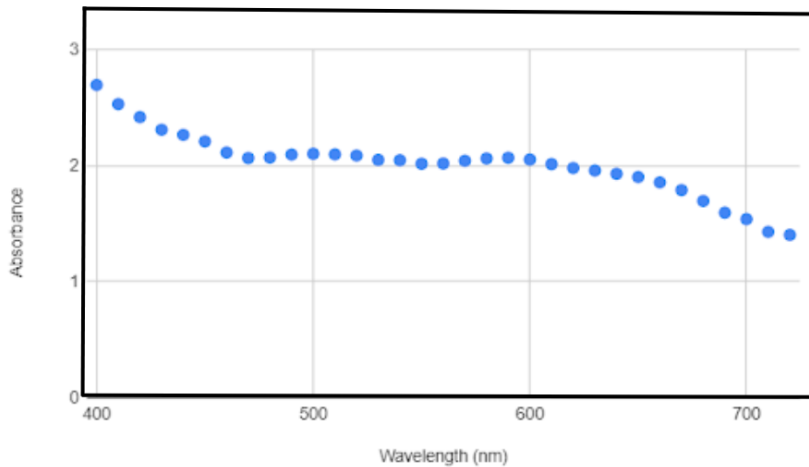


Figure 4.3: Measured absorbance of ND filter with OD of 2

4.1.4 Calibration Curves

First, the linearity check of all 4 sensors was carried out to verify that the signals vary linearly with ISO and exposure time while clicking the picture. A random monochromator wavelength was fixed and the image was taken by varying the ISO and exposure time to arrive at the following graphs. (see figure 4.4 and 4.5) This process was repeated for all four sensors.

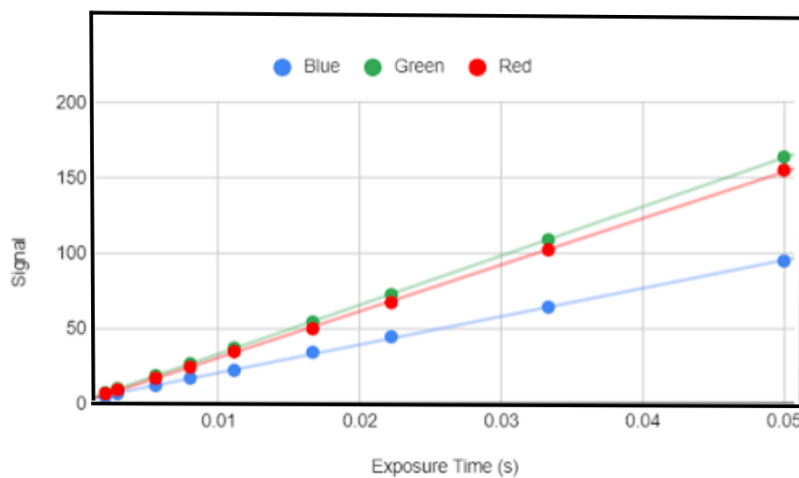


Figure 4.4: Exposure Time Linearity Check of Sensor 3

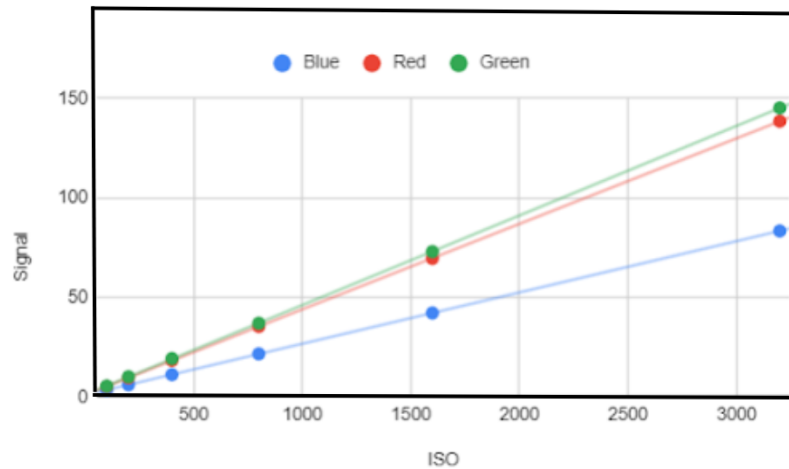


Figure 4.5: ISO Linearity Check of Sensor 3

White balance is another parameter that is user controlled. The following graph (see figure 4.6) shows the variation of signal intensity with changing white balance randomly, keeping ISO and exposure time the same.

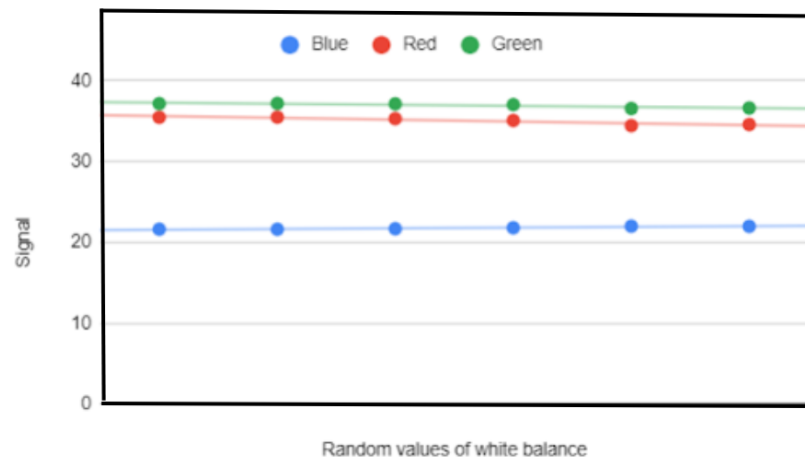


Figure 4.6: White Balance Linearity Check of Sensor 3

This confirmed that white balance doesn't affect the raw signal and it matters in post-processing of the image. After verification of linearity, the spectral response curves were found for all camera sensors.

For comparative study:

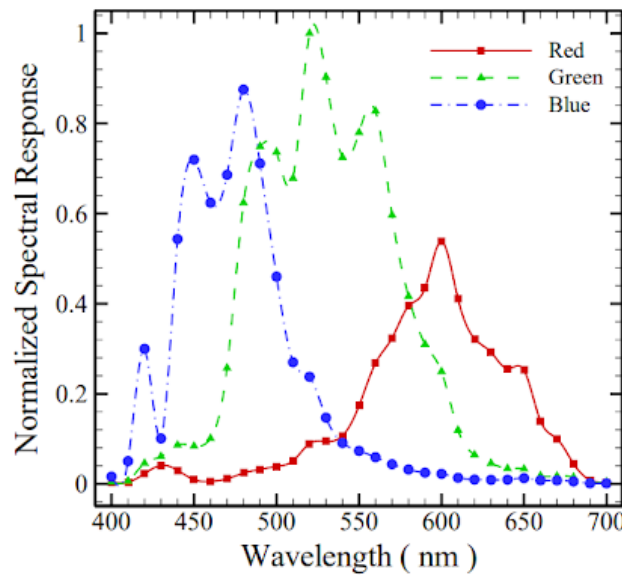


Figure 4.7: Spectral Response curve of CANON EOS 550D camera [1]

Following are the results of the calibration process. As we can see, the curves of the different sensors almost overlap with minor changes. Figure 4.12 shows a sample image of a monochromatic light captured by sensor 2.

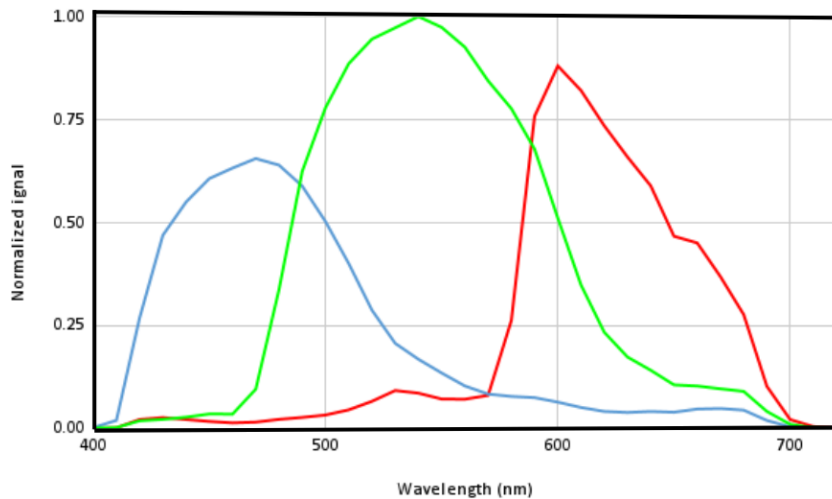


Figure 4.8: Spectral Response Curve of Sensor 1

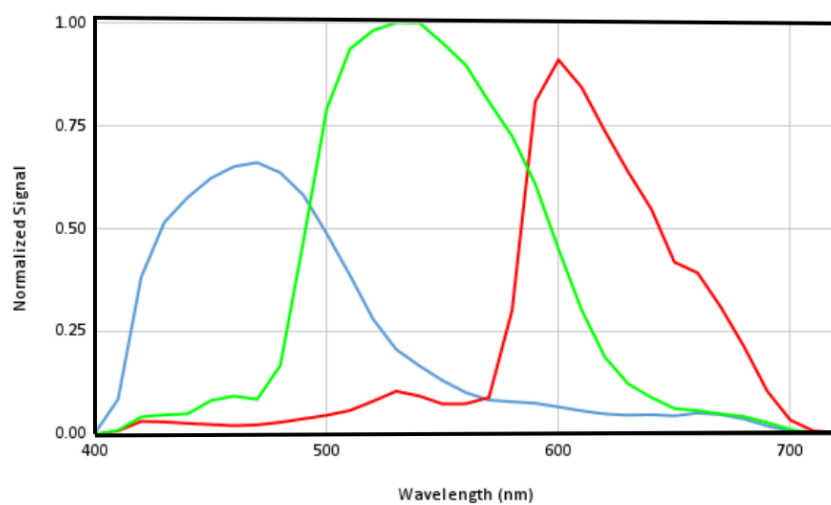


Figure 4.9: Spectral Response Curve of Sensor 2

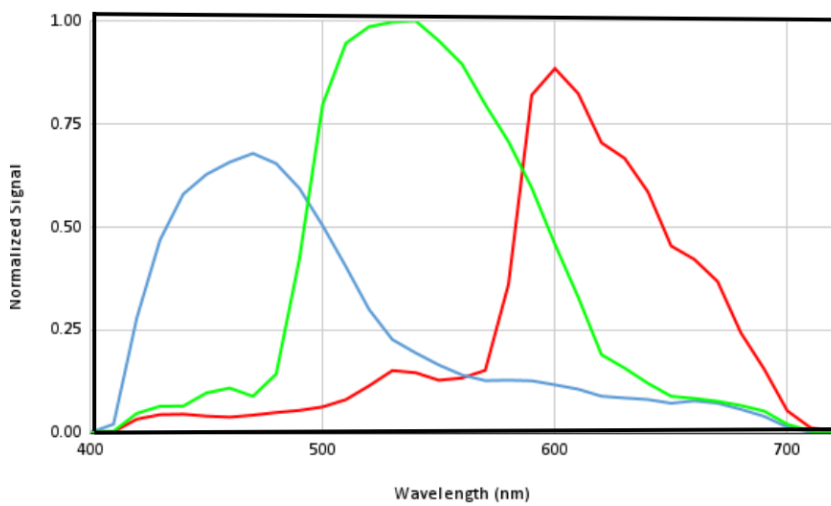


Figure 4.10: Spectral Response Curve of Sensor 3

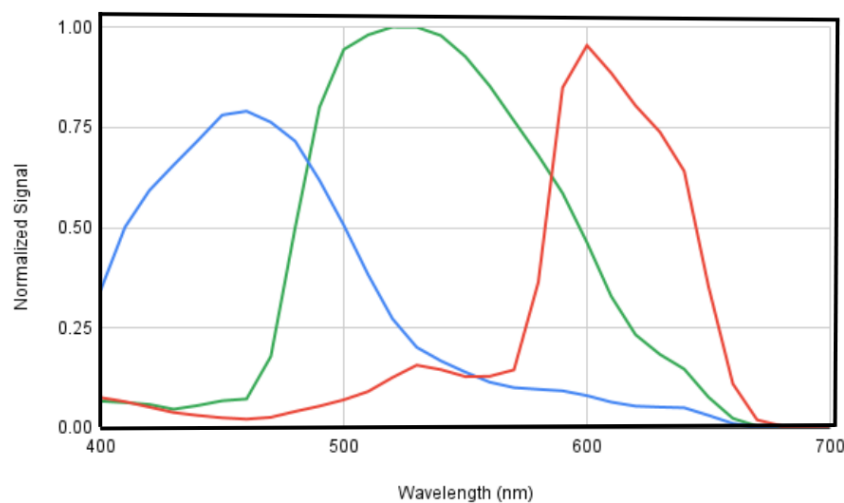


Figure 4.11: Spectral Response Curve of Sensor 4

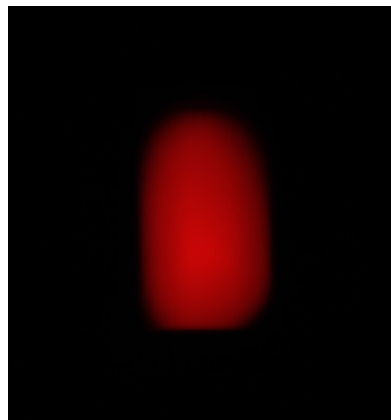


Figure 4.12: Monochromator light captured by Sensor 2

Once these curves are obtained, they are related to the temperature using equation 2.4. For generating soot lookup tables, the soot emissivity was assumed to vary as λ^α where α is known as the soot dispersion exponent. Soot can be categorised as nascent and mature. The soot from a diffusion flame like candle or droplet,.. the value of soot dispersion exponent, α can be taken as 1.38, as the soot is predominantly mature. [1] Similarly, the α value of 4 is assigned to premixed flat flame as soot particles are mostly nascent.

4.2 Candle Flame setup

After calibration of the sensors, the CRP technique was first tested on a candle flame. A MATLAB code was written to convert the raw data from a DNG image (in the case of a phone sensor) or RAW file (in the case of an RPi camera sensor) to temperature. (see Appendix A) The flame temperature was measured using both CRP and B-type thermocouple. The candle flame was radially symmetric and the projected intensities were measured. To find the radial distribution of temperature, Abel Inversion is necessary. [36]

Abel inversion is a mathematical technique used to retrieve the original distribution or profile of a quantity from its integral or projection data. It is particularly useful in tomography and imaging applications, where only the integrated measurements are

available.

To find the actual temperature of a candle flame using 2D data, Abel inversion can be employed to reconstruct the temperature profile within the flame based on the measured projections. The principle behind Abel inversion is based on the Abel transform, which relates the integral measurements of a quantity to its radial distribution. [37] Figure 4.14 shows the first implementation of CRP technique on a candle flame. Abel transform was not implemented in the code. Figure 4.15 gives the distribution of temperature along horizontal axis through the centre of flame. We can see some noise in the data, but a clear trend. Here X-axis is the ordinate of pixel on the fixed row and Y axis shows the temperature. To avoid repetition, the results from other camera sensors are omitted.

For Comparison: Here (a) is with Abel inversion and (b) is without.

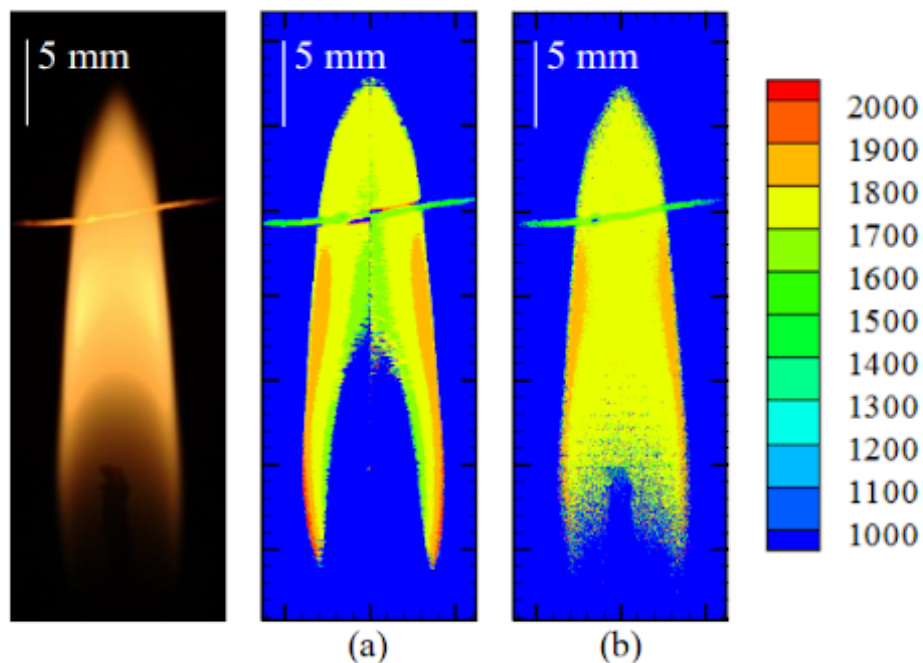


Figure 4.13: CRP Results using Canon EOS 550D [1]

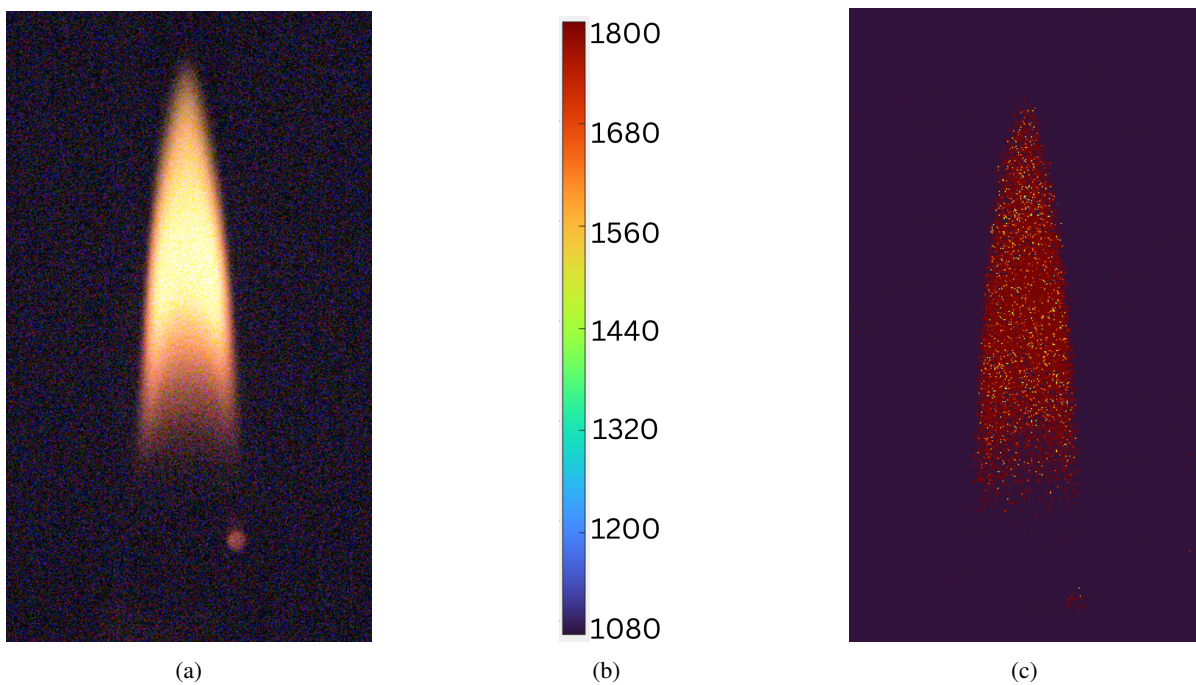


Figure 4.14: Candle flame image and the temperature distribution without Abel inversion

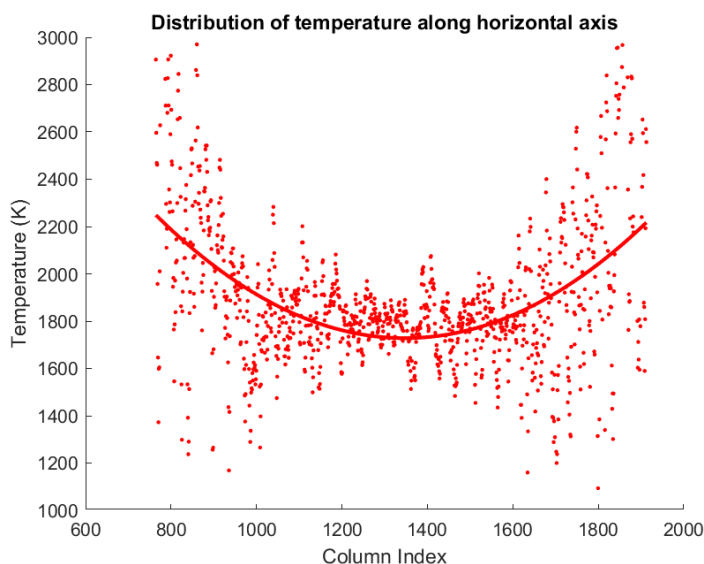


Figure 4.15: Distribution of temperature along horizontal axis through the centre of flame

4.3 Blackbody Furnace Setup

A blackbody furnace, also known as a blackbody source or blackbody radiator, is a specialized instrument used for calibrating and measuring temperatures. It is designed to emit thermal radiation with a known and stable spectral distribution, making it an essential tool for industries and research fields where accurate temperature

measurement is crucial.

The concept of a blackbody refers to an object that absorbs all incident electromagnetic radiation and emits radiation at all wavelengths and intensities, solely based on its temperature. While it is practically impossible to achieve a perfect blackbody in reality, blackbody furnaces aim to approximate this behavior as closely as possible.

Blackbody furnaces consist of a high-temperature cavity or enclosure made of a material with excellent thermal and radiative properties, such as graphite or ceramic. The interior surfaces of the cavity are carefully designed and coated to enhance radiation absorption and minimize reflections. The cavity is typically heated using electrical resistance heaters or other heat sources to reach high temperatures.

The fundamental principle behind a blackbody furnace is that it reaches a state of thermal equilibrium, where the energy absorbed from the heating source is equal to the energy radiated. At this equilibrium, the blackbody furnace emits thermal radiation according to Planck's law, which describes the spectral distribution of radiation emitted by an object based on its temperature.

To calibrate temperature sensors or instruments, they are exposed to the radiation emitted by the blackbody furnace. By measuring the intensity of the radiation and comparing it to the known spectral distribution at a given temperature, accurate temperature calibration can be achieved. This process is commonly performed using radiation thermometers or other devices specifically designed for this purpose. [38]

Calsys 1500 BB blackbody furnace (see figure 4.16) was attempted to be used to obtain the colour ratio against temperature curves of a blackbody source as verification of calibration of sensors. But, the data couldn't be gathered because of the issue with furnace heaters.



Figure 4.16: Calsys 1500BB Blackbody Furnace [39]

4.4 Flat Flame Setup

The McKenna burner, also known as the flat flame burner, is a type of laboratory burner used for various applications, including heating, sterilization, and combustion experiments. It is named after its inventor, Thomas McKenna, an Irish chemist who developed the burner in the early 20th century.

The distinguishing feature of the McKenna burner is its flat flame, which is achieved by utilizing a specially designed burner head. The burner head consists of a horizontal slit or orifice through which a mixture of fuel and air is introduced. The fuel and air are carefully adjusted to achieve a stoichiometric or near-stoichiometric ratio, ensuring efficient and complete combustion.

When the fuel-air mixture exits the orifice, it forms a thin, flat flame that is suitable for a wide range of laboratory applications. The flat flame produced by the McKenna burner is characterized by its high temperature and low luminosity. The McKenna

burner is commonly fueled by natural gas or propane, although other gases can also be used depending on the specific requirements. The burner may incorporate an adjustable control valve to regulate the gas flow rate, allowing precise control over the flame temperature. Additionally, the air supply can be adjusted using a separate control valve to optimize the fuel-air ratio for optimal combustion.

One advantage of the McKenna burner is its simplicity and ease of use. It is relatively inexpensive, and its design allows for a stable, uniform flame that can be easily manipulated for different experimental needs. The burner is often used in laboratory settings, especially in fields such as chemistry, biochemistry, and materials science.

In the McKenna burner, the premixer plays a crucial role in achieving the desired fuel-air mixture before it is introduced into the burner head. The premixer is a component that combines the fuel gas and the air in the correct proportions to ensure efficient and complete combustion.

The premixer is typically located at the junction where the fuel inlet and the air inlet meet. It is designed in a way that promotes thorough mixing of the fuel and air streams, ensuring that they are uniformly combined before reaching the burner head.

In some variations of the McKenna burner, a shroud gas, such as nitrogen, can be used in addition to the fuel and air mixture. The role of the shroud gas is primarily to provide a protective or inert environment around the flame, serving various purposes depending on the specific application. [40] [41]

The roles of shroud gas include:

- Flame Stabilization
- Heat Shielding
- Oxidation Control
- Sample Protection

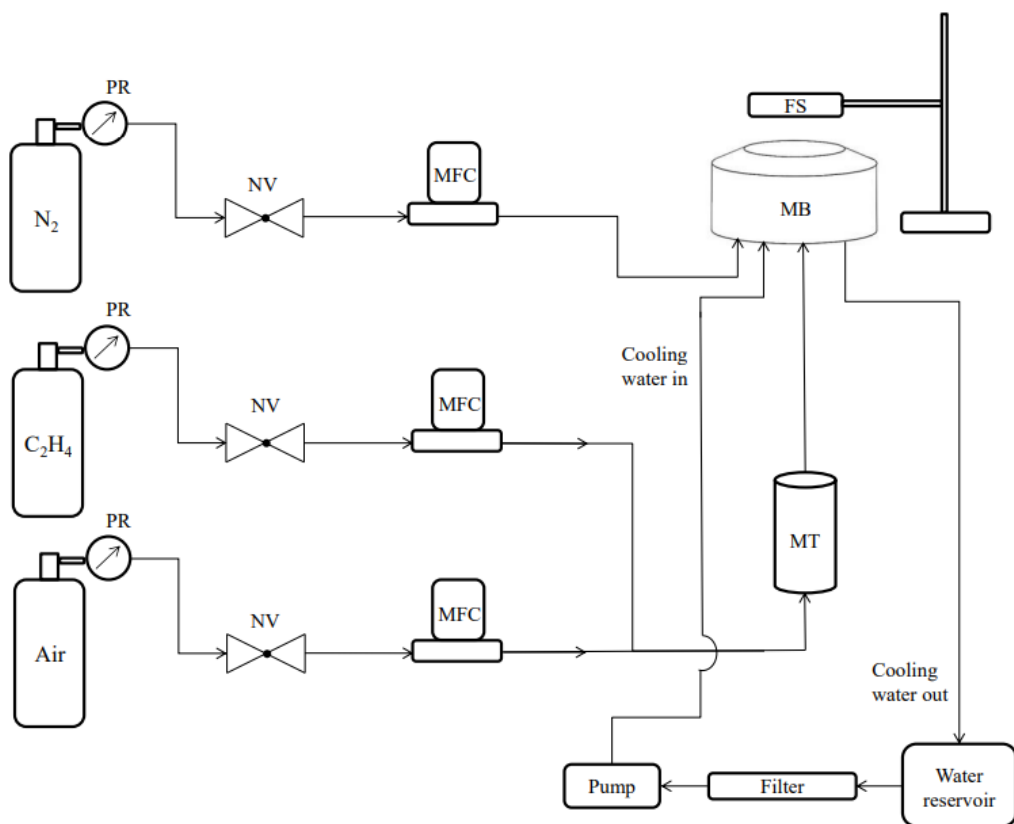
In a fuel-rich McKenna flame, a flame stabilizer is often used to enhance the stability and characteristics of the flame. The flame stabilizer is a component or feature designed to improve the performance of the flame under fuel-rich conditions. Its role can be summarized as follows:

- Flame Structure: In a fuel-rich flame, the excess fuel can lead to a highly reducing environment, which may result in a weak or unstable flame. The flame stabilizer helps to establish and maintain a well-defined flame structure. It promotes proper mixing and combustion of the fuel-rich mixture, ensuring a stable and efficient flame.
- Flame Holding: Fuel-rich flames can be prone to flickering, lifting, or extinguishing due to insufficient air supply. The flame stabilizer helps to hold the flame in place by creating localized recirculation zones or barriers that prevent the flame from being easily extinguished or disrupted. It provides a more consistent and reliable flame, particularly in situations where the air supply may be limited or variable.
- Heat Transfer: The flame stabilizer can influence the heat transfer characteristics of the fuel-rich flame. It may enhance heat transfer from the flame to the surrounding environment or direct the flow of hot gases to specific areas. This can be beneficial in applications where controlled heat distribution or targeted heating is desired.

The schematic of the flat flame burner used [42] can be seen in figure 4.17.

Specifications used for the experiments for the equivalence ratio of 2.3:

- Flow rate of ethylene: 1.39 lpm
- Flow rate of zero air: 8.61 lpm
- Flow rate of nitrogen: 4.14 lpm
- Flow rate of water: 0.9 lpm (Pump used: Crompton Aquagold 100-33 1 HP Single Phase Water Motor Pump)



PR: Pressure Regulator

NV: Needle Valve

MFC: Mass Flow Controller

MB: McKenna Burner

MT: Mixing Tube

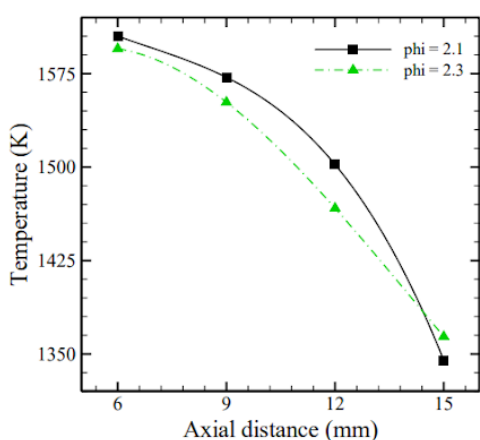
Water reservoir

Filter

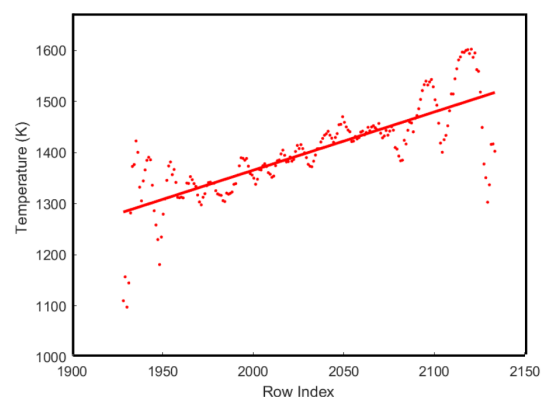
Pump

Figure 4.17: Mckenna Burner Schematic [2]

For comparison:



(a) Results from the CRP using Canon EOS 400D [1]



(b) Variation of temperature along the vertical axis passing through the center

Figure 4.18: Variation of temperature along vertical axis of flat flame

Results:

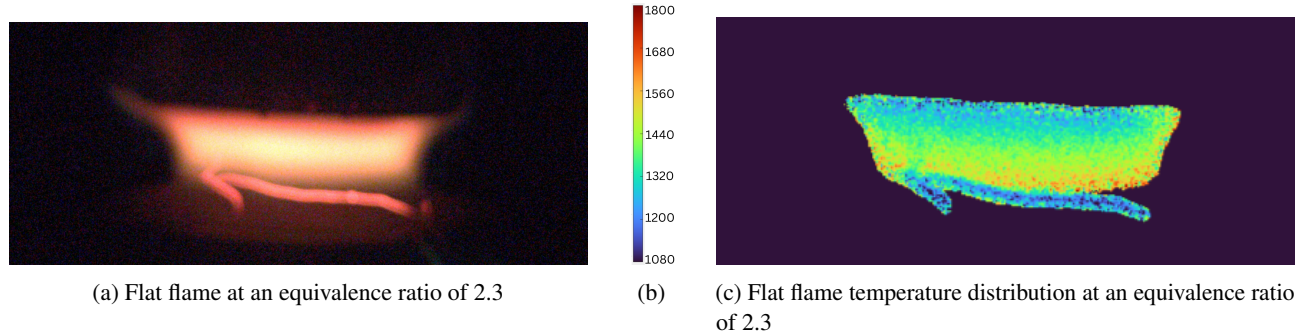


Figure 4.19: Flat flame and the temperature distribution

Figure 4.18 gives the comparison of vertical flame temperature distribution inside the flat flame. The temperature measured by the Canon camera (left) and Sensor 3 (right) is plotted. In plot (a), the X axis is the distance from the bottom of the flame, whereas the X axis in plot (b) is the abscissa of the pixel. Similarly, figure 4.19 shows the image of the flat flame along with the processed image of the temperature distribution. We can also see a B-type thermocouple placed inside the flame.

To verify the results, the simulation for the adiabatic flame temperature at constant pressure (hp model) was performed in NASA CEA to obtain figure 4.20 and the results are compared with the practical data (see table 4.1):

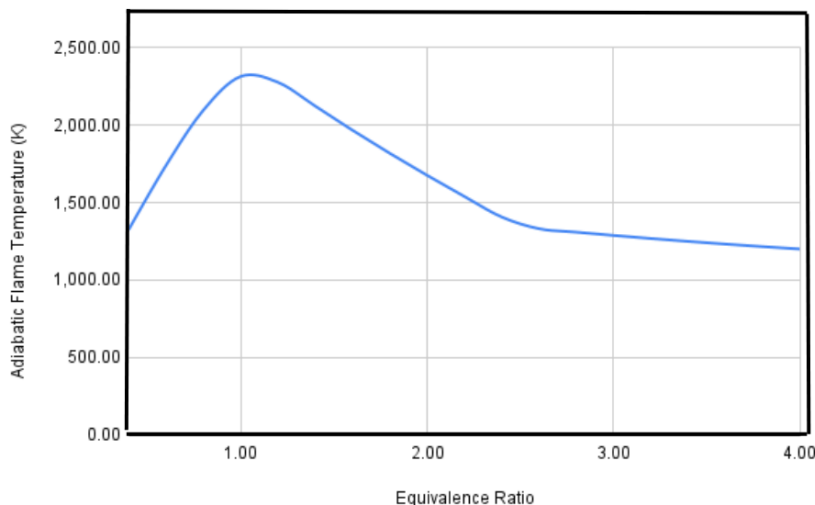


Figure 4.20: NASA CEA simulation results- a variation of adiabatic flame temperature with equivalence ratio

Table 4.1: Variation in flame temperature with equivalence ratio

| Equivalence Ratio | Median temperature along vertical axis (in K) | Mean temperature along vertical axis (in K) | Expected adiabatic flame temperature (in K) |
|--------------------------|--|--|--|
| 2.1 | 1420 | 1425 | 1550 |
| 2.3 | 1395 | 1400 | 1450 |
| 2.5 | 1375 | 1385 | 1400 |

The temperature at equivalence ratio 2.3, at the middle of the flame, was also verified with the B-type thermocouple and it came out to be 1420 K, thus further verifying the CRP procedure.

The ideal flow rate of shield gas, nitrogen in the setup was set to 4.14 l/min, which is equal to the cold flow velocity of the fuel-air mixture whose total flow rate was maintained at 10l/min. [1] But, there was an issue with flame stability. Hence, the flow rate of nitrogen was varied in the range of 0 to 10 l/min and the flame structure and temperature were observed.

The transition as the variation in the flow rate of nitrogen can be seen in figure 4.21.

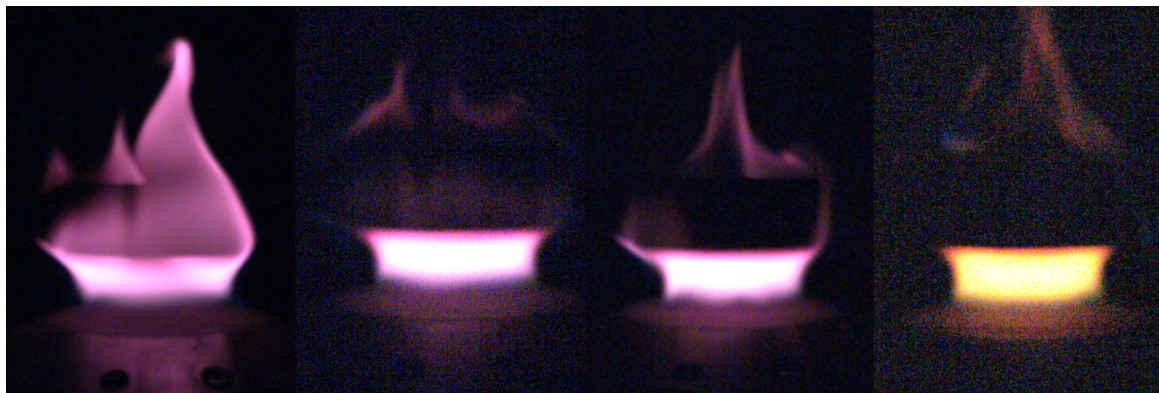


Figure 4.21: Change in flame structure with variation in shield gas flow rate (lpm): 2.5, 5, 7.5, 10

After analyzing the flame temperature statistics of these flames, it was found that the nitrogen flow rate did not impact the flame temperature profile much, although with a low flow rate of nitrogen, the temperatures on the edges of the flame increased because of interaction with the surrounding air. But, its impact on the mean or median

flame temperature was negligible. The structure of the flame was affected majorly by the shield gas flow rate as at high flow rates, it tried to stop the flame from spreading out and pushed it inside.

One limitation of the method is that it doesn't work on non-sooty flame. This was verified when the equivalence ratio was changed to 1.5. (see figure 4.22) The temperature profile for this type of flame came out to be erroneous because the major emission source shifted from soot particle emissions to chemiluminescence. To avoid repetition, the results from other camera sensors are omitted.



Figure 4.22: Blue flat flame with an equivalence ratio of 1.5

4.5 Droplet setup

The droplet combustion setup is one more setup used for the experimental validation of the CRP method. [43] Two fuels, coal tar pitch, a solid fuel and RP1 surrogate fuel, a liquid fuel were used for the experiments.

Coal tar pitch was melted using a hotplate and the quartz rod was dipped in it. Then the rod was inserted inside the combustion chamber and it was ignited using a spark. In the case of RP1 surrogate fuel, a syringe was used to deposit a fuel droplet onto the tip of the quartz rod, which had an approximate diameter of $300 \mu\text{m}$, which was placed inside the combustion chamber. To initiate ignition, a spark was generated by

an ignition transformer. [1]

Following are the results obtained. Figure 4.23 shows the images of the droplet flames of coal tar pitch and RP1 surrogate fuel. Figure 4.24 shows the temperature distribution inside these flames. This is an example of how this method can be used to measure the temperature of a novel fuel with ease.

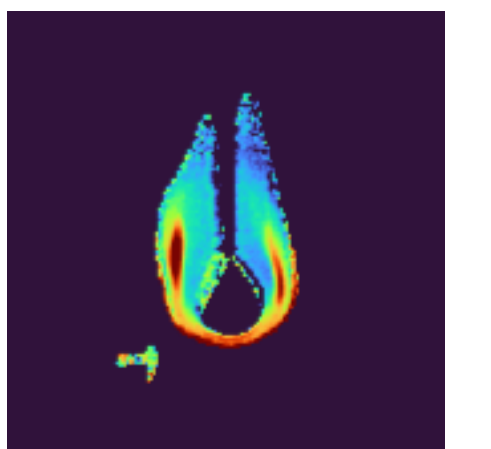


(a)

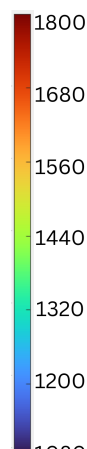


(b)

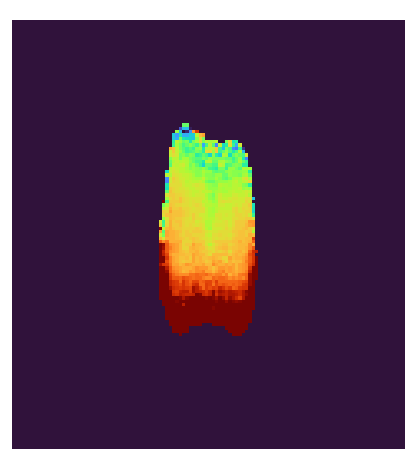
Figure 4.23: The raw phone camera images of coal tar pitch and RP1 surrogate fuel droplet flame



(a)



(b)



(c)

Figure 4.24: Temperature distribution of coal tar pitch flame and RP1 surrogate fuel flame

4.6 Dry Block thermocouple calibration setup

A dry block calibrator, also known as a dry well calibrator, is a temperature calibration instrument used to verify and calibrate temperature sensors and probes. It is commonly employed in various industries, including manufacturing, pharmaceuticals, food processing, and scientific research, where accurate temperature measurements are critical.

The primary function of a dry block calibrator is to generate a stable and precisely controlled temperature environment for testing and calibration purposes. Unlike other calibration methods that involve liquid baths or ovens, a dry-block calibrator uses a solid metal block with precision-drilled wells or inserts to hold the temperature sensors. [44]

The metal block, typically made of aluminum or stainless steel, is designed to have excellent thermal conductivity, allowing for rapid and uniform heat transfer to the temperature sensors. The block is heated or cooled using an internal heating element or Peltier cooling system, depending on the model. The temperature control mechanism is controlled by a microprocessor-based controller, ensuring accurate and stable temperature control within the desired range.

To use a dry block calibrator, the temperature sensors or probes to be calibrated are inserted into the wells of the block. The sensors make direct contact with the metal block, allowing for efficient heat transfer and accurate temperature measurement. The block is then heated or cooled to the desired setpoint temperature. The temperature readings from the sensors under test are compared to the reference temperature displayed on the calibrator's control panel. Any deviations or discrepancies can be noted, and necessary adjustments or calibrations can be made to ensure the accuracy of the sensors.



Figure 4.25: Fluke Calibration 9173 dry-block calibrator [45]

In this study, Fluke Calibration 9173 (see figure 4.25) was used to calibrate N-type and K-type thermocouples. DT 9828 Data Acquisition (DAQ) Module was used to log data to a computer.

Both the thermocouples showed a very good match till 700 degrees Celsius, the maximum temperature of the dry block calibrator. The maximum observed error was 5 degrees Celsius at the highest temperature. But, when the thermocouples were tested on the candle, N type sheathed thermocouple was saturated at around 900 degrees Celsius and the K-type unsheathed thermocouple was saturated at 1200 degree Celsius. Both these values are below the actual candle flame temperature and hence only a precalibrated B-type thermocouple was used for further measurements.

Chapter 5

Product development

Three different platforms were explored initially for the development of a user-friendly product that will process the raw flame image captured by a phone to give the temperature distribution in the flame.:

- **Android Studio Code:** Android Studio is a widely used integrated development environment (IDE) for Android app development. Android Studio supports Java, Kotlin, and C++ programming languages and offers a rich set of libraries and resources for creating Android apps with various functionalities.
- **MIT App Inventor:** MIT App Inventor is a platform developed by the Massachusetts Institute of Technology (MIT) that allows users to create Android

applications without requiring extensive coding knowledge. It follows a visual programming approach, where users can design the app's interface and functionality by arranging blocks of code that represent different actions and behaviors.

- **MATLAB Simulink Android Support Package:** The Simulink Android Support Package provides functionality to develop Android applications using MATLAB and Simulink. It allows users to design algorithms and models in MATLAB/Simulink, and then generate code that can be deployed on Android devices. However, integrating MATLAB code with Android apps can sometimes be challenging, and this approach may require additional troubleshooting and optimization.

Considering the challenges faced with integrating MATLAB code in Android, an alternative solution was explored using MATLAB App Designer. MATLAB App Designer is a graphical development environment within MATLAB that allows users to create apps with a user-friendly interface. With MATLAB App Designer, one can design the app's layout, add interactive components, and write code using MATLAB's programming language. Once the app is designed, one can extract it in various forms, such as a standalone executable or a web app, depending on the requirements.

By exploring MATLAB App Designer, it became possible to leverage the capabilities of MATLAB while simplifying the integration process and potentially overcoming the challenges faced with the Simulink Android Support Package. Since all the processing in the CRP model was done using Matlab in our case, MATLAB App Designer was decided as the final option for developing the app.

In addition to the development of the application using various platforms mentioned earlier, an independent product was created using a Raspberry Pi (RPi) camera module V2 sensor. This product was designed to provide a more generalized solution for colour ratio pyrometry.

Colour ratio pyrometry involves analyzing the raw image captured by a phone's camera to measure temperatures based on colour ratios. However, the challenge is

that each phone's camera has its own unique characteristics and colour representation, which requires individual calibration for accurate temperature measurement.

To address this issue, an independent product was developed using a Raspberry Pi camera sensor. The Raspberry Pi is a small and affordable computer that can be connected to a camera module. By using the RPi camera sensor, the product ensures consistent and standardized image capture across different devices.

With the independent product, the colour ratio pyrometry algorithm can be applied to the raw images captured by the RPi camera sensor. Since the sensor and camera module are the same across all devices, the need for individual calibration for each phone is eliminated. This allows for a more generalized approach where the same calibration parameters can be used across multiple devices, making the temperature measurements more accurate and reliable.

5.1 Milestones in the product development process

5.1.1 Applications developed while learning

Various apps were developed while learning different platforms. These include a unit converter, mathematical operations performer and camera preview app created with Android Studio, a colour detection and another unit converter app developed using MATLAB Simulink, and a checklist app created using MIT App Inventor. (see figure 5.1) Each app serves a specific purpose and showcases the capabilities of the respective development platforms. These helped in gaining familiarity with the different platforms and comparing them in terms of their merits and demerits.

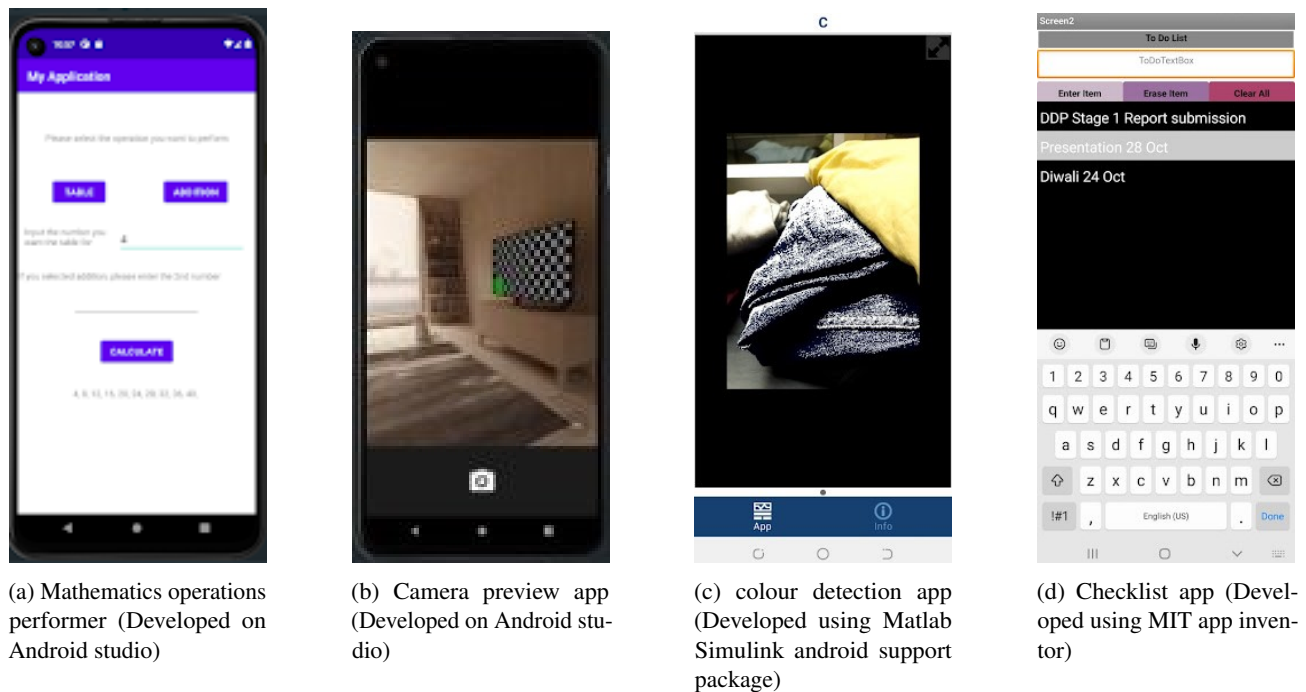


Figure 5.1: Applications created while learning the various methods of android app development

5.1.2 Models worked on while learning

1. Deep learning - This was developed on the MATLAB-Simulink platform. This basic deep-learning model takes an image as input and gives the annotated image as the output. (see figure 5.2)

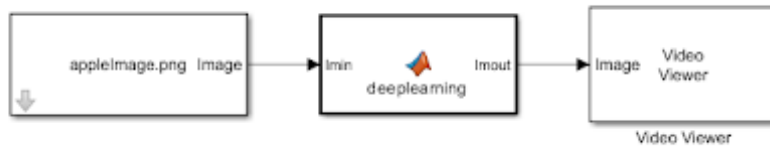


Figure 5.2: Deep learning on Android application using MATLAB Simulink

2. Digit Prediction - This was also developed using the MATLAB-Simulink platform. This can be developed further into an android app. This uses the OpenCV toolbox. This is a model which uses the device camera and predicts the digit using image processing and machine learning. (see figures 5.3 5.4)

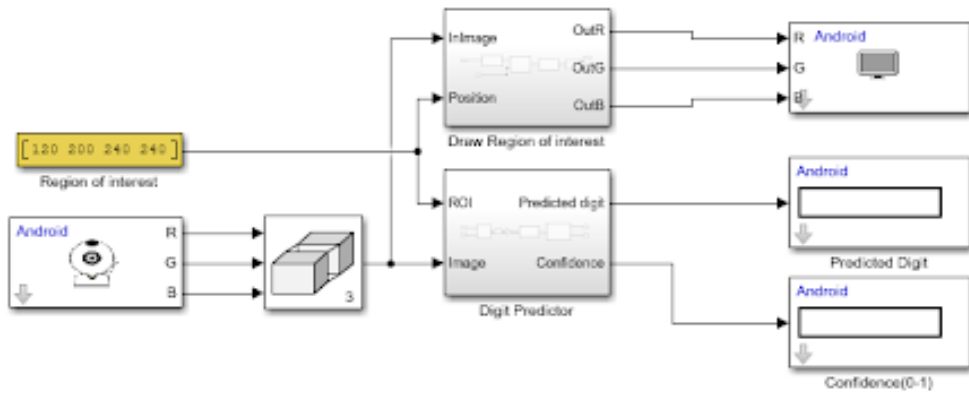


Figure 5.3: Digit Prediction on Android application using MATLAB Simulink-block1



Figure 5.4: Digit Prediction on Android application using MATLAB Simulink-block2

5.2 RPi Product

The RPi product encountered multiple challenges during its development. The Raspberry Pi (RPi) device didn't have the capability to produce images in the DNG format, which was initially desired. Eventually a workaround was found where the images were successfully extracted in more commonly used format, JPEG, with unused RAW data hidden inside.

Another problem was related to the hardware specifications of the RPi used. The specific version used, RPi 3A with 500MB RAM, wasn't powerful enough to handle the requirements of the final RPi Python code. Additionally, due to a shortage of available RPi devices in the market [46], the developed Python code for the final product couldn't be executed on the RPi as intended, although the same can be executed on other versions of Rpi.

To work around this, the final RPi Python code developed was run on a computer instead. As a result, the image captured with the RPi could be processed on a more capable computer. With a stronger RPi, the product could be a standalone solution that performs all necessary operations on the device itself.

The Python program to capture raw images on the raspberry pi and convert them into the required DNG format can be found in Appendix B.

5.3 Final application

Initially, the plan was to develop an Android app using MATLAB Simulink and Android Studio. The vision for this app was to allow users to capture an image and choose manual settings for sensor thresholds, maximum and minimum temperatures, and other parameters. The app would then display a colour map representing the temperature distribution and provide options to download the results. The calibration data specific to the device would be saved within the app for future use. (see figure 5.5)

However, integrating MATLAB Simulink with Android Studio proved to be challenging, as mentioned earlier. As a result, the envisioned app couldn't be developed at that time. Nevertheless, it is important to note that with the necessary expertise in app development, such a product could be a possibility in the future.

A MATLAB application was created using MATLAB App Designer as the final product for colour ratio pyrometry. The purpose of this application is to process images and calculate temperature profiles based on the colour ratios obtained from the image.

To use the application, users need to provide two inputs: a photograph and an Excel file containing calibration data specific to the device being used. The application then performs various processing steps, including extracting data from the image,

demosaicing which is extracting R, G and B matrices from the raw image data and calculating temperatures using the colour ratio pyrometry method.

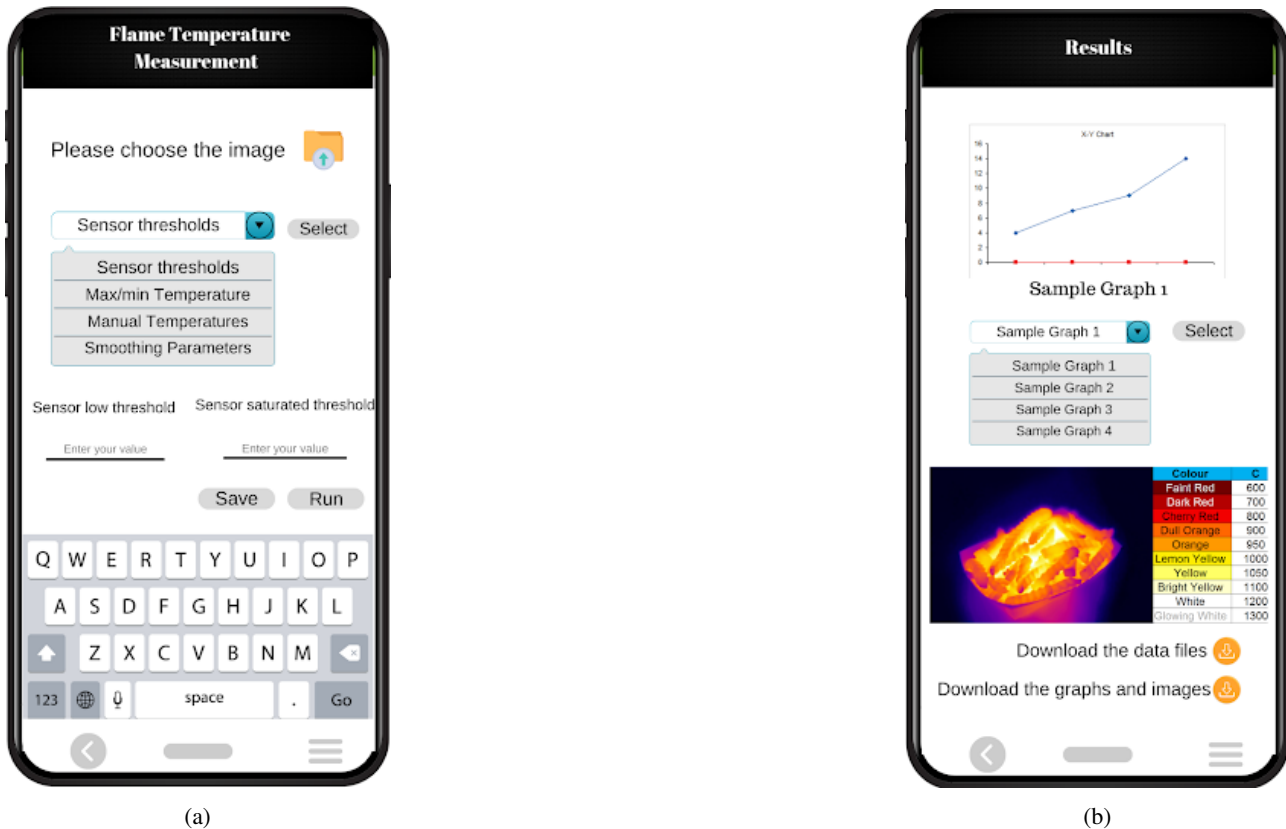


Figure 5.5: Future possibility of advanced Android App

The output of the application is a colour map that displays the temperature profile across the flame. This map provides a visual representation of the temperature distribution. The MATLAB application can be extracted in different forms such as a MATLAB app, a web app, or a standalone application, depending on the user's preference.

In this case, a web app has been developed, which allows users to access and use the application through a web browser. This simplifies the usage of the application as it can be accessed from any device with an internet connection. The web app provides a user-friendly interface for uploading the image and Excel file, performing the processing, and visualizing the temperature map. (see figures 5.6 5.7 5.8)

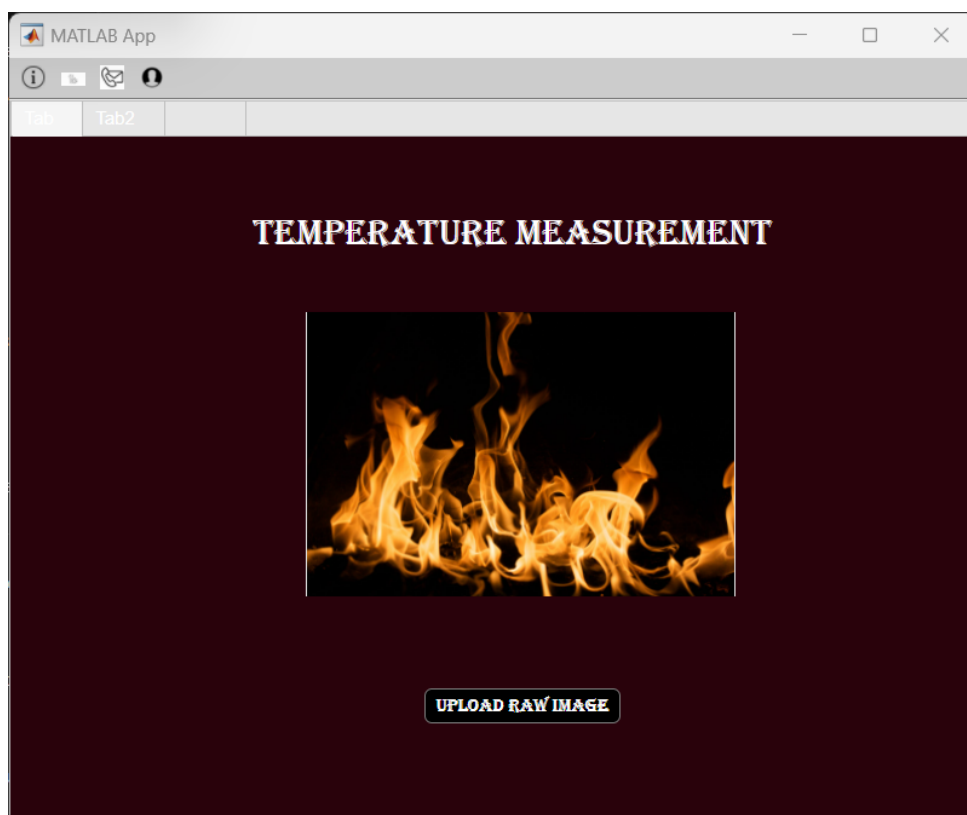


Figure 5.6: Screen 1 of the Matlab app

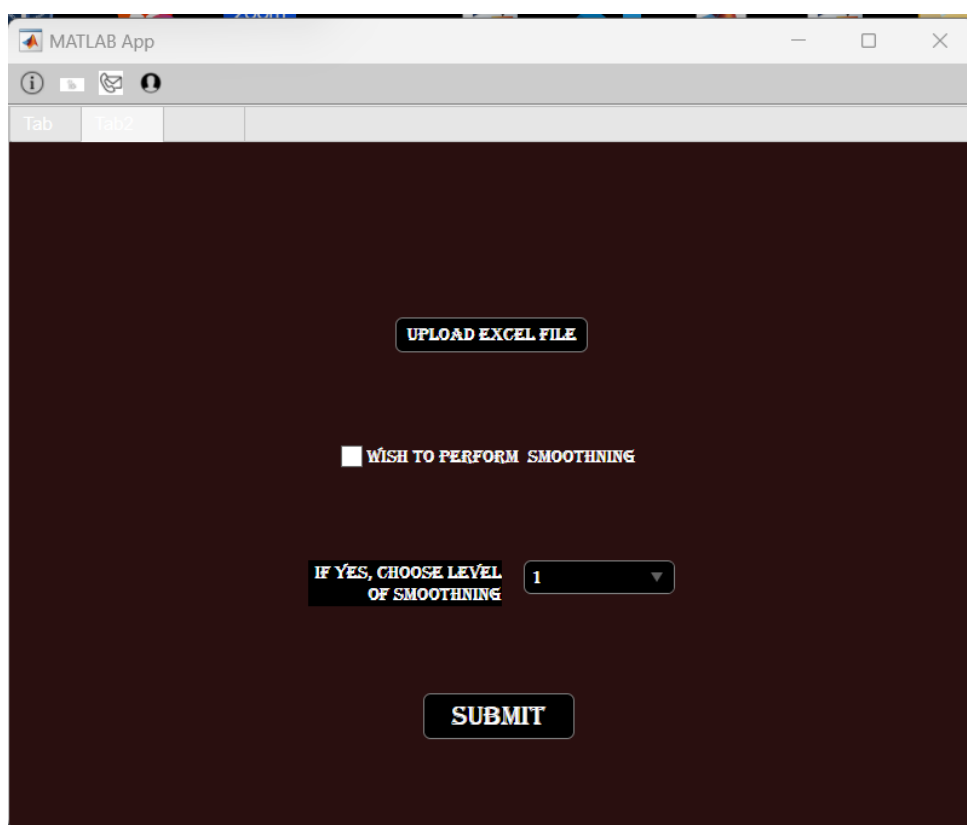


Figure 5.7: Screen 2 of the Matlab app

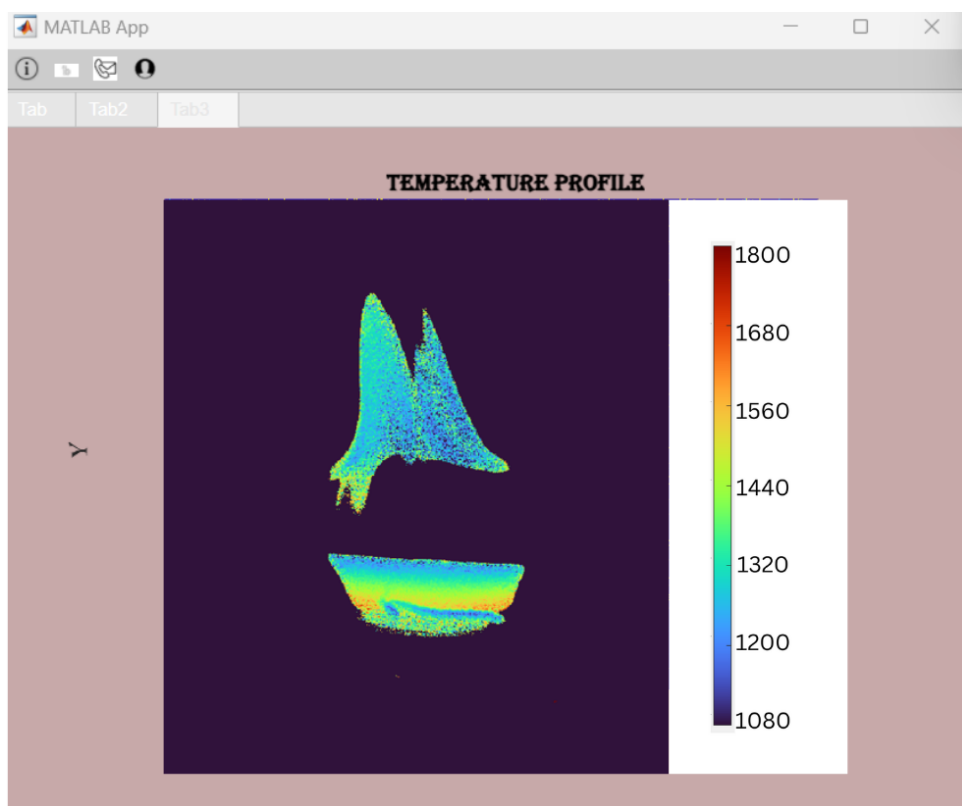


Figure 5.8: Result page of the Matlab app

Chapter 6

Conclusions

The aim of the project was to develop the CRP procedures for smartphone camera images, verifying them using experiments and building a user-friendly product out of it.

The literature review provided valuable insights into the measurement techniques and imaging technology used for flame temperature analysis. The technique of colour ratio pyrometry was thoroughly studied and the mathematical formulation was converted into Matlab and Python codes with few extra requirements.

The practical implementation of the colour ratio pyrometry method demonstrated its effectiveness in analyzing flame temperatures. The method was tested on candle flame,

Mckenna burner flame and droplet flame and the average error in the temperature measured came out to be less than 80K. (<5%)

It was also compared with the already implemented CRP technique using a DSLR camera and the results matched well. The developed Matlab app-based product showcased the easy-to-use and very affordable practical application of the research findings.

The current study is limited to symmetric and sooty flames. A hurdle between the prototype and the product of this application is the need to calibrate every new sensor and the phone sensors are upgrading rapidly. Hence, an RPi-based product was also realized where the camera module can be kept constant and the product can be reproduced in large quantities.

In the future, this research can be extended to make a generalized model for all kinds of flames, including asymmetric and non-sooty flames. One probable way for CRP measurements of non-sooty flames is by introducing a few soot or other solid particles in them. To get the radial distribution of temperature in the case of radially symmetric flames, the Abel inversion algorithm can be implemented in the future to make the results more useful. Also, the technique can be extended to get the soot fraction in the flame.

Appendices

Appendix A

A.1 Matlab code for CRP

A.1.1 Part 1 of the code

```
clear all  
filename= "D:\DDPData\Test Data and Codes\Blackbody\ForTempCodeAnmol.  
xlsx";  
alpha= 4; %For Flat Flame  
%alpha= 1.38 %For Candle Flame  
[b_by_r_arr, g_by_r_arr, b_by_g_arr]= AlgoForTempCandle(filename,alpha);  
  
%Inputs  
folder= "D:\DDPData\Test Data and Codes\ImagesToProcess\Anmol";  
flag_smooth=1;  
smooth_filter_sz= 5;  
  
Files= dir(folder + "\*.dng");  
for k= 1:length(Files)  
    Filenames= Files(k).name;  
end  
  
ETcol=[];  
ISOcol=[];  
WhiteLev=[];  
SS=[];  
FocalLength=[];  
minArr=[];  
maxArr=[];
```

```

for mm =1:length(Files)
    newfilename = fullfile(folder, Files(mm).name); % Put file name here
    rawImg = double(imread(newfilename));
    meta_info = imfinfo(newfilename);
    ISO=meta_info.DigitalCamera.ISOSpeedRatings;
    ET= meta_info.DigitalCamera.ExposureTime;
    ShutterSpeed=meta_info.DigitalCamera.ShutterSpeedValue ;
    Focus=meta_info.DigitalCamera.FNumber ;
    White=meta_info.WhiteLevel ;
    highestPixel= (max(max(rawImg)));
    lowestPixel= (min(min(rawImg)));

```

% ----- Linearize

```

black = 0;
saturation = White; % can be done ourself, overexposure.
lin_bayer = (rawImg-black)/(saturation-black);
lin_bayer = max(0,min(lin_bayer,1)); % Keeping values between 0 and 1

```

% ----- Demosaicing

```

temp = uint16(lin_bayer*(2^16));
lin_rgb_full = single(demosaic(temp,'bggr'))/65536;
%Nikhil grbg
%Sagar gbrg
%Anmol bggr

```

% ----- Smoothening

```

if(flag_smooth)
    H = fspecial("average",smooth_filter_sz);

```

```

linS_rgb(:,:,1) = imfilter(lin_rgb_full(:,:,1), H, "replicate"); % R Layer
Smoothening
linS_rgb(:,:,2) = imfilter(lin_rgb_full(:,:,2), H, "replicate");
linS_rgb(:,:,3) = imfilter(lin_rgb_full(:,:,3), H, "replicate");
tag_filter = "Smooth";
else
    linS_rgb = lin_rgb_full;
    tag_filter = "Unsmooth";
end

[row, col, ~] = size(linS_rgb);
R = zeros(row, col);
G = zeros(row, col);
B = zeros(row, col);

for i = 1:row
    for j = 1:col
        R(i,j) = linS_rgb(i,j,1);
        G(i,j) = linS_rgb(i,j,2);
        B(i,j) = linS_rgb(i,j,3);
    end
end

for a= 1:size(B,1)
    for b=1:size(B,2)
        if B(a,b)+G(a,b)+R(a,b)<0.01
            B(a,b)=0;
        end
    end
end

B_by_G=zeros(size(B,1),size(B,2));

```

```

B_by_R= zeros(size(B,1),size(B,2));
G_by_R= zeros(size(B,1),size(B,2));

for c= 1:size(B,1)
    for d=1:size(B,2)
        B_by_R(c,d)= B(c,d)/R(c,d);
        G_by_R(c,d)= G(c,d)/R(c,d);
        B_by_G(c,d)= B(c,d)/G(c,d);
    end
end

T_arr1= zeros(size(B_by_R,1),size(B_by_R,2));
T_arr3= zeros(size(B_by_G,1),size(B_by_G,2));

for m= 1:size(B_by_R,1)
    for n=1:size(B_by_R,2)
        b_by_r= B_by_R(m,n);
        g_by_r= G_by_R(m,n);
        b_by_g= B_by_G(m,n);
        [T1,T2,T3]= Calculate_Temp(b_by_r_arr, g_by_r_arr, b_by_g_arr,
        b_by_r, g_by_r, b_by_g);
        T_arr1(m,n)=T1;
        T_arr3(m,n)=T3;
    end
end

outputDir = 'D:\DDPData\Test Data and Codes\ImagesToProcess\Nikhil';
T1fileName = string(newfilename) + 'T1.csv';
T2fileName = string(newfilename) + 'T2.csv';
writematrix(T_arr1, T1fileName);
writematrix(T_arr3, T2fileName);

```

```

ETcol(mm)=ET;
ISOcol(mm)=ISO;
minArr(mm)=lowestPixel;
maxArr(mm)=highestPixel;
SS(mm)=ShutterSpeed;
WhiteLev(mm)= White;
FocalLength(mm)= Focus;
disp(mm);

end
A= cat(1, ETcol, ISOcol, SS, WhiteLev, FocalLength, minArr, maxArr);
MetaInfofileName= "FileInfo2_MetaInfo.csv";
writematrix(A,MetaInfofileName)

```

A.1.2 Part 2

clear all

```

folder= "D:\DDPData\Test Data and Codes\ImagesToProcess\Anmol";
Files= dir(folder+ "\*.csv");
for k= 1:length(Files)
    Filenames= Files(k).name;
end

medianval=[];
meanval=[];
minval=[];
maxval=[];
medianval2=[];
meanval2= [];
minval2= [];
maxval2= [];
for mm =1:length(Files)

```

```

file= fullfile(string(folder),Files(mm).name);
T_arr = readmatrix(file);
figure;
imshow(uint8(T_arr/12));
axis on;
colormap("turbo");
colorbar;
clim([90 150])
saveas(gcf, sprintf('Temperature Distribution' + string(Files(mm).name)+ '.png') );
close(figure)

% Plot T1 array
figure;
imshow(T_arr, []);
title('T1 Array');
% Select a point on the plot
disp('Please select a point on the plot of T1.');
[x, y] = ginput(4); % Choose a point by clicking on the figure
close(figure)

% Get the column index corresponding to the selected point
columnIndex = round(x(1));

% Get the T1 values along the selected column
columnValues = T_arr(y(1):y(2), columnIndex);
% Filter the array to keep only the non-zero elements
nonZeroValues= find(columnValues ~= 0);
nonZeroElements = columnValues(columnValues ~= 0);

% Calculate the median of the non-zero elements
medianValue = median(nonZeroElements);

```

```
meanValue = mean(nonZeroElements);
minvalue= min(nonZeroElements);
maxvalue= max(nonZeroElements);

% Select the range of X values for the curve
x_range= [y(1),y(2)];

% Extract the X and Y values within the selected range
x_range_values = y(1)+ nonZeroxValues-1;
y_range_values = nonZeroElements;

% Perform quadratic curve fitting
degree = 1; % Quadratic curve degree
coefficients = polyfit(x_range_values, y_range_values, degree);

% Generate X values for the quadratic curve
x_curve = linspace(min(x_range_values), max(x_range_values), 100);

% Evaluate the quadratic curve using the fitted coefficients
y_curve = polyval(coefficients, x_curve);

% Reduce the size of scatter points
markerSize = 5; % Adjust marker size as needed
% Plot scatter curve with T1 values along the selected column
figure;
scatter(nonZeroxValues+y(1)-1, nonZeroElements,markerSize,'filled', 'red');
hold on;
plot(x_curve, y_curve, 'red', 'LineWidth', 2);
xlabel('Row Index');
ylabel('Temperature (K)');
title('Distribution of temperature along vertical axis');
% Save the scatter plot with an appropriate name
```

```
saveas(gcf, sprintf('Vertical Distribution of Temperature'+ string(Files(mm)).  
name)+ '.png') );  
close(figure)  
  
% Get the column index corresponding to the selected point  
rowIndex = round(y(3));  
  
% Get the T1 values along the selected column  
rowValues = T_arr(rowIndex,x(3):x(4));  
% Filter the array to keep only the non-zero elements  
nonZeroValues2= find(rowValues ~= 0);  
nonZeroElements2 = rowValues(rowValues ~= 0);  
  
% Calculate the median of the non-zero elements  
medianValue2 = median(nonZeroElements2);  
meanValue2 = mean(nonZeroElements2);  
minvalue2= min(nonZeroElements2);  
maxvalue2= max(nonZeroElements2);  
  
% Select the range of X values for the quadratic curve  
x_range2 = [x(3), x(4)]; % Example range from X = 3 to X = 8  
  
% Extract the X and Y values within the selected range  
x_range_values2 = x(3)+ nonZeroValues2-1;  
y_range_values2 = nonZeroElements2;  
  
% Perform quadratic curve fitting  
degree2 = 2; % Quadratic curve degree  
coefficients2 = polyfit(x_range_values2, y_range_values2, degree2);  
  
% Generate X values for the quadratic curve  
x_curve2 = linspace(min(x_range_values2), max(x_range_values2), 100);
```

```
% Evaluate the quadratic curve using the fitted coefficients
y_curve2 = polyval(coefficients2, x_curve2);

% Plot scatter curve with T1 values along the selected column
figure;
scatter(x(3)+ nonZeroXValues2-1, nonZeroElements2,markerSize, 'filled','red
');
hold on;
plot(x_curve2, y_curve2, 'red', 'LineWidth', 2);
xlabel('Column Index');
ylabel('Temperature (K)');
title('Distribution of temperature along horizontal axis');

% Save the scatter plot with an appropriate name
saveas(gcf, sprintf('Horizontal Distribution of Temperature'+ string(Files(mm).
name)+ '.png') );
close(figure)

medianval(mm)=medianValue;
meanval(mm)=meanValue;
minval(mm)=minvalue;
maxval(mm)=maxvalue;
medianval2(mm)=medianValue2;
meanval2(mm)= meanValue2;
minval2(mm)= minvalue2;
maxval2(mm)= maxvalue2;
disp(mm)

end

A= cat(1, medianval, meanval, minval, maxval, medianval2, meanval2, minval2,
maxval2);
fileName= "FileData_Anmol.csv";
writematrix(A,fileName)
```

A.2 Functions used in the code

1. AlgoForTempCandle

```

function [b_by_r, g_by_r, b_by_g] = AlgoForTempCandle(filename,alpha)
    %filename= "D:\DDPData\ForTempCode.xlsx"
    cfa_data= readmatrix(filename);
    %alpha= 4;
    h= 6.626*10^-34;
    c= 3*10^8;
    k= 1.38*10^-23;
    e= 2.7183;
    b_by_r=[];
    g_by_r=[];
    b_by_g=[];
    for T= 1000:10:3000
        sum_r=0;
        sum_b=0;
        sum_g=0;
        for i= 1:1:30
            lambda= (400+10*i-5)*10^-9;
            sum_r= sum_r+ (cfa_data(i+1,1)+cfa_data(i,1))/2*lambda^(-alpha)/lambda^5*((e^(h*c/(lambda*k*T))-1)^(-1))*10*10^-9;
            sum_b= sum_b+ (cfa_data(i+1,2)+cfa_data(i,2))/2*lambda^(-alpha)/lambda^5*((e^(h*c/(lambda*k*T))-1)^(-1))*10*10^-9;
            sum_g= sum_g+ (cfa_data(i+1,3)+cfa_data(i,3))/2*lambda^(-alpha)/lambda^5*((e^(h*c/(lambda*k*T))-1)^(-1))*10*10^-9;
        end
        b_by_r= [b_by_r, 1/(sum_r/sum_b)];
        g_by_r= [g_by_r, 1/(sum_r/sum_g)];
        b_by_g= [b_by_g, 1/(sum_g/sum_b)];
    end
end

```

2. CalculateTemp

```

function [T_b_by_r, T_g_by_r, T_b_by_g] = Calculate_Temp(b_by_r_arr,
g_by_r_arr, b_by_g_arr, b_by_r, g_by_r, b_by_g)
T= 1000:10:3000;
if b_by_r ~= 0
    T_b_by_r= linear_interp(b_by_r_arr, T, 201, b_by_r);
    T_g_by_r=linear_interp(g_by_r_arr, T, 201, g_by_r);
    T_b_by_g=linear_interp(b_by_g_arr, T, 201, b_by_g);
else
    T_b_by_r= 0;
    T_g_by_r=0;
    T_b_by_g=0;
end
end

```

```

function interp_val = linear_interp(n_values, T, n, new_val)
% n_values: array of n monotonously increasing values
% n: number of values in n_values array
% new_val: value to interpolate

```

```

% find the index of the element in n_values that is just less than new_val
ind = find(n_values < new_val, 1, 'last');

```

```

% if new_val is smaller than the smallest value in n_values, return the first
element in n_values
if isempty(ind)
    interp_val = 0;
    return
end

```

```
% if new_val is larger than the largest value in n_values, return the last
element in n_values
if ind == n
    interp_val = 0;
    return
end

% perform linear interpolation
interp_val = T(ind) + (new_val - n_values(ind)) * (T(ind+1) - T(ind)) / (
n_values(ind+1) - n_values(ind));

end
```

Appendix B

B.1 RPi code to capture raw image

1. RPi code to capture raw image:

```
raspistill -r -o image.jpg
```

2. RPi code to convert a raw image to CSV file:

```
from picamraw import PiRawBayer, PiCameraVersion
import matplotlib.pyplot as plt
import numpy as np
import os
for j in range(3):
    i= 200+100*j
    raw_image_path = os.path.join(os.path.expanduser('~'), 'Desktop\\RPi
camera calib\\v2', 'image590test1ss1000iso'+str(i) +'.jpg')
    csv_file_path = os.path.join(os.path.expanduser('~'), 'Desktop\\RPi
camera calib\\v2', 'image590test1ss1000iso'+str(i) +'.csv')

raw_bayer = PiRawBayer(
    filepath=raw_image_path, # A JPEG+RAW file, e.g. an image
    captured using raspistill with the "--raw" flag
    camera_version=PiCameraVersion.V2,
    sensor_mode=0
)
print(raw_bayer.bayer_array.shape) # A 16-bit 2D numpy array of the
bayer data
print(raw_bayer.bayer_order) # A 'BayerOrder' enum that describes the
arrangement of the R,G,G,B pixels in the bayer_array
```

```
raw_bayer.to_rgb() # A 16-bit 3D numpy array of bayer data collapsed  
into RGB channels (see docstring for details).  
raw_bayer.to_3d() # A 16-bit 3D numpy array of bayer data split into  
RGB channels (see docstring for details).  
np.savetxt(csv_file_path, raw_bayer.bayer_array, delimiter=',')
```

All other codes and documentation can be found on the GitHub page of the author.

Appendix C

C.1 Edge Detection

To pinpoint the precise location of the flame in the image, object detection is necessary. Microsoft created the Visual Object Tagging Tool (VoTT), a free and open-source electron application for labeling and annotating images. YOLO is another well-known tool for object identification. YOLO, or you only look once, is an acronym. It is a group of object detectors with a single deep-learning step. They are capable of more than just accurate, real-time object detection. Once the flame is identified, we may crop the image just to use the necessary portion, preventing mistakes.

Yovo V5 model was trained on around 60 online flame images and was implemented to detect flame in the picture. The accuracy was not so good as the dataset was limited. Later, this task was achieved by different simple technique that is based on the sum of R, G and B values at the pixel. If this sum is less than a predetermined threshold, it is concluded that the said pixel is dark or there is no flame at that pixel.

Bibliography

- [1] Anand Sankaranarayanan et al. “Investigation of sooting flames by color-ratio pyrometry with a consumer-grade DSLR camera”. In: *Review of Scientific Instruments* 92.4 (2021), p. 044905. DOI: 10.1063/5.0018353. eprint: <https://doi.org/10.1063/5.0018353>. URL: <https://doi.org/10.1063/5.0018353>.
- [2] Md. Saif Ansari. “Sooty Flame Temperature Measurement using Smartphone and DSLR Camera powered by Color Ratio Pyrometry Technique”. MA thesis. Department of Mechanical Engineering Indian Institute of Technology, Bombay Powai - 400076, Maharashtra, India: Indian Institute of Technology, Bombay, June 2022.
- [3] P. R. N. Childs, J. R. Greenwood, and C. A. Long. “Review of temperature measurement”. In: *Review of Scientific Instruments* 71 (Aug. 2000), pp. 2959–2978. DOI: 10.1063/1.1305516.
- [4] Gavin Sutton. “The development of a combustion temperature standard for the calibration of optical diagnostic techniques”. In: (2007).
- [5] *File:Thermocouple circuit Ktype including voltmeter temperature.svg*. https://en.m.wikipedia.org/wiki/File:Thermocouple_circuit_Ktype_including_voltmeter_temperature.svg. Last accessed on: 2023-06-22.
- [6] Gavin Sutton et al. “A combustion temperature and species standard for the calibration of laser diagnostic techniques”. In: *Combustion and Flame* 147 (2006), pp. 39–48. DOI: <https://doi.org/10.1016/j.combustflame.2006.07.013>. URL: <https://www.sciencedirect.com/science/article/pii/S0010218006001842>.
- [7] *Simultaneous coherent anti-Stokes Raman scattering and two-dimensional laser Rayleigh thermometry in a contained technical swirl combustor*. <https://opg.optica.org/ao/fulltext.cfm?uri=ao-34-15-2780&id=45681>. Last accessed on: 2023-06-22.
- [8] G Hartung, J Hult, and C F Kaminski. “A flat flame burner for the calibration of laser thermometry techniques”. In: *Measurement Science and Technology* 17 (Aug. 2006), p. 2485. DOI: 10.1088/0957-0233/17/9/016. URL: <https://dx.doi.org/10.1088/0957-0233/17/9/016>.
- [9] Chandra Shakher and Anil Kumar Nirala. “A review on refractive index and temperature profile measurements using laser-based interferometric techniques”. In: *Optics and Lasers in Engineering* 31.6 (1999), pp. 455–491. DOI: [https://doi.org/10.1016/S0143-8166\(99\)00037-8](https://doi.org/10.1016/S0143-8166(99)00037-8). URL: <https://www.sciencedirect.com/science/article/pii/S0143816699000378>.
- [10] *Michelson interferometer*. https://en.wikipedia.org/wiki/Michelson_interferometer. Last accessed on: 2023-06-22.
- [11] *Thin filament pyrometry*. https://en.wikipedia.org/wiki/Thin_filament_pyrometry. Last accessed on: 2023-06-22.
- [12] L. P. Goss et al. “Thin-Filament Pyrometry: A Novel Thermometry Technique for Combusting Flows”. In: *Journal of Engineering for Gas Turbines and Power* 111.1 (Jan. 1989), pp. 46–52. DOI: 10.1115/1.3240226. URL: <https://doi.org/10.1115/1.3240226>.
- [13] J. Thevenet, M. Siroux, and Bernard Desmet. “Brake disc surface temperature measurement using a fiber optic two-color pyrometer”. In: Jan. 2008. DOI: 10.21611/qirt.2008.02_12_14.
- [14] Jay Polk et al. “Scanning optical pyrometer for measuring temperatures in hollow cathodes”. In: *The Review of scientific instruments* 78 (Oct. 2007), p. 093101. DOI: 10.1063/1.2774828.

- [15] Shawn A. Reggeti, Ajay K. Agrawal, and Joshua A. Bittle. “Two-color pyrometry system to eliminate optical errors for spatially resolved measurements in flames”. In: *Appl. Opt.* 58 (Nov. 2019), pp. 8905–8913. DOI: 10.1364/AO.58.008905. URL: <https://opg.optica.org/ao/abstract.cfm?URI=ao-58-32-8905>.
- [16] H. C. Hottel and F. P. Broughton. “Determination of True Temperature and Total Radiation from Luminous Gas Flames”. In: *Industrial & Engineering Chemistry Analytical Edition* 4.2 (1932), pp. 166–175. DOI: 10.1021/ac50078a004. eprint: <https://doi.org/10.1021/ac50078a004>. URL: <https://doi.org/10.1021/ac50078a004>.
- [17] Martin H. Davy et al. “Two-Colour Pyrometry Measurements of Low-Temperature Combustion using Borescopic Imaging”. In: *SAE WCX Digital Summit*. SAE International, Apr. 2021. DOI: <https://doi.org/10.4271/2021-01-0426>. URL: <https://doi.org/10.4271/2021-01-0426>.
- [18] John M. Densmore et al. “High-speed digital color imaging pyrometry”. In: *Appl. Opt.* 50.17 (June 2011), pp. 2659–2665. DOI: 10.1364/AO.50.002659. URL: <https://opg.optica.org/ao/abstract.cfm?URI=ao-50-17-2659>.
- [19] *Chemeurope*. https://www.chemeurope.com/en/encyclopedia/Wien_approximation.html. Last accessed on: 2022-10-21.
- [20] Blair C. Connelly et al. “Two-Dimensional Soot Pyrometry with a Color Digital Camera”. In: 2005.
- [21] Vinay Raj and S. Prabhu. “Measurement of surface temperature and emissivity of different materials by two-colour pyrometry”. In: *The Review of scientific instruments* 84 (Dec. 2013), p. 124903. DOI: 10.1063/1.4847115.
- [22] *What is a Sensor?* <https://www.sensorcleaning.com/whatisasensor.php>. Last accessed on: 2023-06-22.
- [23] *Types of Camera Sensors*. <https://www.photometrics.com/learn/camera-basics/types-of-camera-sensor>. Last accessed on: 2022-10-21.
- [24] *CCD vs. CMOS*. <https://www.teledynedalsa.com/en/learn/knowledge-center/ccd-vs-cmos/>. Last accessed on: 2023-06-22.
- [25] *Bayer filter*. https://en.wikipedia.org/wiki/Bayer_filter. Last accessed on: 2023-06-22.
- [26] *X-Trans CMOS Continuous Evolution on Resolution and Color Reproduction*. <https://fujifilm-x.com/global/products/x-trans-cmos/>. Last accessed on: 2023-06-22.
- [27] *What is a DSLR (Digital SLR) Camera?* <https://photographylife.com/what-is-a-dslr>. Last accessed on: 2023-06-22.
- [28] *Camera sensor*. <https://unsplash.com/s/photos/camera-sensor>. Last accessed on: 2022-06-22.
- [29] *FOCUSING MODES EXPLAINED – UNDERSTANDING CAMERA AUTOFOCUS MODES*. <https://capturetheatlas.com/focus-modes/>. Last accessed on: 2023-06-22.
- [30] *Camera2 overview*. <https://developer.android.com/training/camera2>. Last accessed on: 2022-10-21.
- [31] *How to Enable Camera2 API and Shoot RAW on Android*. <https://appuals.com/enable-camera2-api-shoot-raw-android>. Last accessed on: 2022-10-21.
- [32] *The Monochromator and Its Role in the Spectrograph*. <https://www.technologynetworks.com/analysis/articles/the-monochromator-and-its-role-in-the-spectrograph-369390#D2>. Last accessed on: 2023-06-22.
- [33] *Spectra UV-VIS-NIR Quasar Series Scientific Monochromators*. https://www.holmarc.com/spectra_UV_VIS_NIR_quasar_series_scientific_monochromators.php. Last accessed on: 2022-06-22.
- [34] *Optical Power Meters*. https://www.rp-photonics.com/optical_power_meters.html. Last accessed on: 2023-06-22.

- [35] *Optical Power Meter OPM Series*. https://www.holmarc.com/optical_power_meter.php. Last accessed on: 2022-06-22.
- [36] Peter B. Kuhn et al. “Soot and thin-filament pyrometry using a color digital camera”. In: *Proceedings of the Combustion Institute* 33 (2011), pp. 743–750. ISSN: 1540-7489. DOI: <https://doi.org/10.1016/j.proci.2010.05.006>.
- [37] Carsten Killer. *Abel Inversion Algorithm*. <https://www.mathworks.com/matlabcentral/fileexchange/43639-abel-inversion-algorithm>. MATLAB Central File Exchange. 2023.
- [38] *Black Body Calibrator*. <https://tempsens.com/blog/black-body-calibrator>. Last accessed on: 2023-06-22.
- [39] *AST CALsys 1500BB*. <https://www.alutal.com.br/en/produto/ast-calsys-1500bb>. Last accessed on: 2022-06-22.
- [40] S. Prucker, W. Meier, and W. Stricker. “A flat flame burner as calibration source for combustion research: Temperatures and species concentrations of premixed H₂/air flames”. In: *Review of Scientific Instruments* 65 (Sept. 1994), pp. 2908–2911. DOI: 10.1063/1.1144637.
- [41] Qi Wu et al. “Simultaneous In-Situ Measurement of Soot Volume Fraction, H₂O Concentration, and Temperature in an Ethylene/Air Premixed Flame Using Tunable Diode Laser Absorption Spectroscopy”. In: *Combustion Science and Technology* 189 (2017), pp. 1571–1590. DOI: 10.1080/00102202.2017.1308358.
- [42] *Flat Flame Burner*. <https://www.flatflame.com/>. Last accessed on: 2022-06-22.
- [43] Anand Sankaranarayanan et al. “Droplet combustion studies on two novel energetic propellants, an RP-1 surrogate fuel, and their blends”. In: *Fuel* 255 (Aug. 2019). DOI: 10.1016/j.fuel.2019.115836.
- [44] *What is a Dry Block? – Parts of the Temperature Calibrator*. <https://instrumentationtools.com/what-is-a-dry-block/>. Last accessed on: 2023-06-22.
- [45] *Fluke Calibration 9173 Field Metrology Well*. <https://www.fluke.com/en-us/product/calibration-tools/temperature-calibrators/fluke-calibration-9173>. Last accessed on: 2022-06-22.
- [46] *Raspberry Pi- Supply chain update – it's good news!* <https://www.raspberrypi.com/news/supply-chain-update-its-good-news/>. Last accessed on: 2023-06-22.